

Spectral fluctuations of multi-parametric complex matrix ensembles: evidence of a single parameter dependence

Mohd. Gayas Ansari and Pragya Shukla

Department of Physics, Indian Institute of Technology, Kharagpur-721302, West Bengal, India

(Dated: March 5, 2024)

We numerically analyze the spectral statistics of the multiparametric Gaussian ensembles of complex matrices with zero mean and variances with different decay routes away from the diagonals. As the latter mimics different degree of effective sparsity among the matrix elements, such ensembles can serve as good models for a wide range of phase transitions e.g. localization to delocalization in non-Hermitian systems or Hermitian to non-Hermitian one. Our analysis reveals a rich behavior hidden beneath the spectral statistics e.g. a crossover of the spectral statistics from Poisson to Ginibre universality class with changing variances for finite matrix size, an abrupt transition for infinite matrix size and the role of complexity parameter, a single functional of all system parameters, as a criteria to determine critical point. We also confirm the theoretical predictions in [1, 2], regarding the universality of the spectral statistics in non-equilibrium regime of non-Hermitian systems characterized by the complexity parameter.

I. INTRODUCTION

Complex random matrices appear as the matrix representations of non-Hermitian operators of complex systems in diverse areas (e.g. see [3, 4, 7–16, 18–44]). A knowledge of their statistical behavior is necessary to determine many of the physical properties. As the degree and type of randomness is often system specific and leads in general to a wide range of ensembles, it is desirable to seek a common mathematical formulation of their statistical behavior; this would not only help to probe a specific complex system but also in revealing the connections hidden underneath among seemingly different complex systems.

The existence of a common mathematical formulation has been indicated in past for the Hermitian operators [45–52] and is also verified by the detailed numerical analysis on many body as well as disordered systems. While a corresponding formulation for the non-Hermitian cases was first derived in [2] and further developed recently in [1] for the average spectral density, its detailed theoretical and numerical analysis on the complex plane e.g. the fluctuations of the radial and angular parts of the eigenvalues, and validity of complexity parameter based predictions was not pursued earlier (mainly due to lack of interest in non-Hermitian operators in past). We note that contrary to Hermitian case, the statistical behavior on the complex plane is far more richer, has many degrees of freedom and therefore technically far more complicated notwithstanding analogous basic mathematical skeletons in both the cases. Intense renewed interest in the statistics of non-Hermitian operators but lack of a theoretical formulation motivates us to pursue, in the present work, a detailed numerical analysis of the fluctuations.

As indicated by detailed theoretical, numerical as well as experimental studies, the statistical behavior of complex systems with ergodic wave dynamics can be well described by basis-invariant random matrix ensembles i.e. those with ensemble density dependent only on the invariant properties of the matrix e.g. trace [5, 6, 43, 52]. In case of non-ergodic wave dynamics, however, the basis details affect the matrix representation of the complex system and lead to basis-non-invariant, multiparametric ensembles of random matrices. As intuitively expected, the details of the ensemble are often sensitive to underlying system conditions but the relevant exact information is usually obscured by underlying complexity leaving access only to some statistical parameters. Fortunately, based on the statistical approaches e.g. maximum entropy hypothesis, a knowledge of such parameters is often sufficient to predict the nature of the distribution e.g. Gaussian if the first two moments of the matrix elements are known. This motivates us to consider a complex system, e.g a Hamiltonian with complicated many body interactions, represented by a complex matrix H in an arbitrary orthonormal basis and with known constraints only on the mean and variances of the matrix elements H_{kl} and their pair wise correlations. Based on the maximum entropy hypothesis (MEH), it can then be described by an ensemble of $N \times N$ complex matrices H defined by a Gaussian ensemble density

$$\tilde{\rho}(H, y, x) = C \exp \left[- \sum_{s=1}^2 \sum_{k,l} (y_{kl;s} H_{kl;s}^2 + x_{kl;s} H_{kl;s} H_{lk;s}) \right] \quad (1)$$

with C as the normalization constant, y and x as the sets of variances and covariances of various matrix elements, and, the subscript s on a variable refers to one of its components, i.e real ($s = 1$) or imaginary ($s = 2$).

For an ensemble to be an appropriate representation of the physical system of interest, the ensemble parameters must be chosen as the functions of system parameters. As the ensemble parameters $y_{kl;s}, x_{kl;s}$ in eq.(1) can be arbitrarily chosen (including an infinite value for non-random entries), this enables $\rho(H, y, x)$ to represent a large class of non-Hermitian matrix ensembles e.g. varying degree of sparsity or bandedness. Further by a variation of $y_{kl;s}, x_{kl;s}$, eq.(1) can also be used as a model to analyze a wide range of crossovers/ transitions e.g. from Hermitian to non-Hermitian system conditions, from one non-Hermitian universality class to another one e.g. Poisson to Ginibre universality class [1, 2].

The standard route for the statistical analysis of a random matrix ensemble is based on the fluctuation measures of its eigenvalues and eigenfunctions and requires, in turn, a knowledge of their joint probability distribution function (JPDF). An integration of the latter over undesired variables then, in principle, leads to the correlation functions for the remaining variables e.g. the spectral correlations resulting from an integration over all eigenfunction components. The integration is technically easier if the ensemble density is basis invariant e.g. depends only on the trace of the matrix [52]. Except for the basis invariant cases, an integration of the ensemble density is in general technically complicated and a search for alternative routes is necessary. As discussed in [1, 2], a differential equation for the spectral JPDF for non-Hermitian multiparametric Gaussian ensembles can be derived from the ensemble density. An integration of this equation over all eigenvalues except one of them then leads to parametric evolution equation for the spectral density in the complex plane; the solution of the equation under certain approximations and its verification by numerical analysis was discussed in [1]. But, contrary to the spectral density, a derivation of its local fluctuation

measures from the spectral JPDF equation is not an easy task and requires theoretical approximations. (Indeed, this is also the case for the Hermitian ensembles: although the technical complexity here is relatively lower due to real eigenvalues, theoretical formulations are known either for second order spectral correlations for a few initial conditions or BBGKY hierarchical correlations among all orders [43, 48, 52, 54]).

To gain an insight about the relevant theoretical approximation, it is instructive to first pursue a numerical investigation of the spectral fluctuations for the basis-dependent ensembles of complex matrices. While the topic is rich in unknown vistas, we confine our focus in the present work on following objectives:

- (i) to establish whether the fluctuation measures satisfy local ergodicity assumption (needed to approximate spectral averages by the ensemble ones),
- (ii) to analyze crossover of the fluctuation measures between Poisson and Ginibre universality class with varying ensemble parameters,
- (iii) to analyze size-dependence of the fluctuation measures and seek critical spectral statistics,
- (iv) to verify that different ensembles exhibit same spectral statistics if their complexity parameters are same and if they have same initial conditions.

The motivation for the first objective arises from the rich physics reported for non-Hermitian many body systems with non-ergodic dynamics. The ergodic dynamics is a necessary tool for system's approach to thermalization and thereby permitting application of standard statistical tools e.g. equivalence assumption of spectral with ensemble averages. While the spectral density for non-ergodic systems is in general non-ergodic, this does not rule out local ergodicity of local fluctuation measures. and requires a numerical verification. We note that the ergodicity of the local fluctuations mentioned above in (i) is different from the one discussed in [1] in context of the average spectral density.

The necessity for the second objective lies in the unavoidable presence of disorder as well as many body interactions in physical systems which can manifests in a variety of ways in the matrix representation of their non-Hermitian operators; it is natural to query whether presence of disorder with/ without interactions has any, and if so, what impact on the fluctuations of the excitations over representative ensemble and can these fluctuations mimic, at least locally, the fluctuations on a single spectral plane? .

A complex system often acts in an infinite dimensional Hilbert space and the random matrices in its representative ensemble are therefore of infinite size. The numerical analysis however involves only finite size matrices. For application of the numerical information to real systems, it is necessary to analyze how far the approximations and insights based on finite sizes be extended to infinite sizes e.g. due to some scaling relations and is the basis of our third objective.

The quest for the fourth objective originates from the significant claim made in the study [2], indicating the existence of a single parameter governed common evolution equation for the spectral correlations for a wide range of physical systems represented by the Gaussian non-Hermitian random matrix ensembles. The system dependence in the formulation enters through the complexity parameter Y , a function of ensemble parameters and thereby a functional of system parameters [1, 2]. The common evolution equation predicts the analogy of the statistical fluctuations for different non Hermitian Gaussian ensembles if their rescaled Y values as well as the initial conditions are same. This in turn claims an existence of universality in non-equilibrium regime of the ensemble representing a complex system (subjected to random perturbations); the significance of the claim requires therefore a detailed numerical verification.

The paper is organized as follows. As mentioned above, the complexity parameter formulation of the spectral JPDF along with a detailed theoretical and numerical analysis of the average spectral density is discussed in [1]. The present work pursues the study [1] further, extending it to the local spectral fluctuations analysis on the complex plane. To keep the present work self contained, Section II briefly reviews the relevant steps of detailed theoretical formulation derived in [1, 2]. Section III presents the ensemble densities for the cases considered in our numerical analysis. To fulfil our objectives, here we numerically analyze complex matrix ensembles for three different types of off-diagonal variances; the chosen ensembles are special cases of the ensemble density eq.(1). A comparative analysis of the spectral fluctuation measures for different ensembles requires a specific rescaling of the spectrum which in turn depends on whether the spectrum is ergodic or not; this is discussed in section III. A, along with a numerical study of the ergodicity for the three ensembles along with the Ginibre ensembles. Sections III.B and III.C present the numerical analysis of the fluctuations for each of the three ensembles for many system parameters; the objective of these sections is not only to verify that the crossover from initial to stationary state is indeed driven by a single function of all system conditions but also to provide insights about permissible approximations necessary for theoretical analysis of mathematically intractable fluctuation measures. Section III.D presents the details of a critical point analysis of the spectral statistics and reconfirm our theoretical predictions of [1]. We conclude in section IV with a brief reviews of our main results and open questions.

II. COMPLEXITY PARAMETRIC FORMULATION OF SPECTRAL CORRELATIONS

With ensemble (1) representing a non Hermitian operator H in an N -dimensional Hilbert space, a typical matrix $H \equiv [H_{kl}]$ in the ensemble (1) is a $N \times N$ complex matrix. The eigenvalues $\lambda_1, \dots, \lambda_N$ of H are distributed on the complex plane with $\langle U_n |$ and $|V_n \rangle$ as the left and right eigenvectors corresponding to λ_n ($\equiv \lambda_{n1} + i \lambda_{n2}$ with subscripts 1 and 2 referring to real and imaginary parts of the variable),

$$\langle U_n | H = \lambda_n \langle U_n |, \quad H |V_n \rangle = \lambda_n |V_n \rangle. \quad (2)$$

The eigenvectors are defined up to multiplication by scalar constants and are bi-orthogonal i.e $\langle U_m |V_n \rangle = \delta_{mn}$. (A nonhermitian matrix is considered to be diagonalisable except at the exceptional points. The latter are the points in the parameter space at which some of the eigenvalues become degenerate and the corresponding eigenvectors coalesce into one. But the number of such points is at most finite and it is possible to avoid them by considering suitable parametric conditions).

The eigenvalue spectrum is described by the equation $H = U\Lambda V$ with $\Lambda = [\lambda_n \delta_{mn}]$ as the eigenvalue matrix, $U \equiv [U_{kn}]$, $V \equiv [V_{kn}]$ as the left and right eigenvector matrices with $X_{kn} \equiv \langle k | X_n \rangle$ as the entries for $X = U, V$. Following from eq.(1), the matrix elements of H are randomly distributed. This in turn randomizes its eigenvalues and eigenfunctions thus rendering it imperative to consider their distributions. Confining present analysis to eigenvalues only, the joint probability density function $\tilde{P}(z_1, z_2, \dots, z_N)$ (short notation for $P(z_1, z_1^*, \dots, z_N, z_N^*)$, equivalently $P(z_{11}, z_{12}, \dots, z_{N1}, z_{N2})$) for the eigenvalues λ_n to occur at z_n on the spectral plane can be defined as

$$\tilde{P}(z_1, z_2, \dots, z_N) = \int \prod_{s=1}^2 \prod_{n=1}^N \delta(z_{ns} - \lambda_{ns}) \tilde{\rho}(H) DH. \quad (3)$$

with $DH \equiv \prod_{kl;s} dH_{kl;s}$.

An integration of the spectral JPDF over $N-n$ variables z_{n+1}, \dots, z_N leads to the probability densities $R_n(z_1, \dots, z_n; Y)$ at each of the n points z_1, \dots, z_n on the spectral plane irrespective of the rest $N-n$ variable positions. Also referred as n^{th} order spectral density correlator or simply n -level correlation functions, can be defined as

$$R_n(z_1, \dots, z_n) = \frac{N!}{(N-n)!} \int \tilde{P}(z_1, \dots, z_N) D\Omega_{n+1} \quad (4)$$

with $D\Omega_{n+1} \equiv \prod_{k=n+1}^N dz_k dz_k^*$. The case $n = 1$ corresponds to the ensemble averaged spectral density R_1 . Alternatively, assuming the spectral density (defined as $\sigma(z) = \sum_{n=1}^N \delta(z - z_n) \delta(z^* - z_n^*)$) consisting of a secular part superimposed by a fluctuating part i.e $\sigma(z) = \langle \sigma(z) \rangle + \delta\sigma(z)$, R_n can also be defined as the correlation between n -point fluctuations of $\sigma(z)$: $R_n(z_1, \dots, z_n) = \langle \delta\sigma(z_1) \dots \delta\sigma(z_n) \rangle$. (The notation $\rho(z)$ used in the study [1] for the spectral density is replaced here by $\sigma(z)$; this is to avoid confusion with the notation $\rho(H)$ that is used in *appendix A*).

All spectral fluctuation measures can in principle be derived from the set of R_n , thus rendering the latter as the ideal tool for theoretical analysis. But a determination of R_n from eq.(4) requires a multi-dimensional integration besides a prior knowledge of JPDF $\tilde{P}(z_1, z_2, \dots, z_N)$. Fortunately the technical complexity of the multi-dimensional integrals can be circumvented by a differential route [1, 2] that describes the response of the ensemble to varying system conditions (briefly discussed in *appendix A*). As discussed in [1, 2], the analysis leads to a common mathematical formulation of the evolution equation for $P(z_1, \dots, z_N)$ and thereby $R_n(z_1, \dots, z_n)$, as system parameters vary. The evolution of both P as well as R_n on the spectral plane is however governed by a single functional Y of the system parameters (briefly discussed in *appendix A*) [1, 2],

$$\frac{\partial R_n}{\partial Y} = \sum_{s=1}^2 \sum_{j=1}^n \frac{\partial}{\partial z_{js}} \left[\frac{\partial R_n}{\partial z_{js}} - 2 \frac{\partial \ln |\Delta_n(z)|}{\partial z_{js}} R_n - 2 \int_{-\infty}^{\infty} d^2 z_{n+1} R_{n+1} \frac{\partial \ln |z_j - z_{n+1}|}{\partial z_{js}} \right] \quad (5)$$

where $\Delta_n(z)$ is the Vandermonde determinant,

$$\Delta_n(z) \equiv \prod_{k < l}^n (z_k - z_l) \quad (6)$$

and Y is a function of all distribution parameters $x_{kl;s}, y_{kl;s}$. For case $x_{kl;s} \neq 0$, we have [1]

$$Y = \mp \frac{1}{M} \sum_{k,l;s} \ln \left(2(\gamma^2 + 2(-1)^s \tilde{c}_{kl;s} y_{kl;s} + \gamma\sqrt{w})/y_{kl;s} \right) + c_0. \quad (7)$$

with $y_{kl;s} = c_{kl;s} y_{kl;s}$, $w = \gamma^2 + 4y_{kl;s}(c_{kl;s}y_{kl;s} + (-1)^s \tilde{c}_{kl;s})$ and the constants $c_{kl;s}$ and $\tilde{c}_{kl;s}$ given by the relations $x_{kl;s}^2 + (-1)^s \gamma x_{kl;s} - c_{kl;s} y_{kl;s}^2 - (-1)^s \tilde{c}_{kl;s} y_{kl;s} = 0$. Here M is the number of evolving parameters: $M = 2N^2$ for cases with $y_{kl;s} \neq 0$. (We note that, for the cases in which a specific $y_{kl;s} = 0$ throughout the evolution, with k, l, s arbitrary, the number M of evolving parameter is less than $2N^2$). For the case $x_{kl;s} = 0$, we have $c_{kl;s} = 0, \tilde{c}_{kl;s} = 0$ and therefore $w = \gamma^2$; Y in this case is [1, 2]

$$Y = \pm \frac{1}{M} \sum_{k,l;s} \ln y_{kl;s} + c_0, \quad (8)$$

As Y is a function of the ensemble parameters $y_{kl;s}$ and $x_{kl;s}$, hereafter it will be referred as the ensemble complexity parameter. We note that in case of non-Hermitian complex systems (e.g. those with disorder or many body interactions) represented by the ensemble (1), $y_{kl;s}$ and $x_{kl;s}$ are in general functions of the system parameters e.g. disorder, hopping, interactions, dimensionality, boundary and topological conditions; as a consequence Y is a functional of the system parameters. As Y appears as a "time" like parameter in the evolution described by eq.(5), with $Y \rightarrow \infty$ corresponding to its stationary limit, the solution of eq.(5) for finite Y will be referred as the non-stationary or non-equilibrium states of the correlations. Although not relevant for the present study but worth recalling for completeness sake is the following aspect of the evolution of P and thereby R_n in the complex plane: it is subjected to $M - 1$ constants, referred as t_2, \dots, t_M in [1], which in turn depend on the matrix (global) constraints on H and can be chosen e.g. as the functions of the basis parameters (as the evolution of the ensemble density occurs in a fixed basis-space in which the matrix H is represented).

An additional parameter, although not present either in eq.(1) or eq.(4) but appearing in eq.(7), is γ ; it is a measure of the external confining potential, the dynamics is subjected to (discussed in details in section II. A of [1]). But, for R_n describing local spectral correlations in the bulk, the confining potential does not affect them and therefore γ does not appear in eq.(4). As the focus of the present study is an analysis of the bulk correlations (near $z \sim 0$), hereafter we set $\gamma = 1$ in eq.(7) without loss of generality.

As mentioned above, R_n for $n > 1$ describe the local fluctuations of the spectral density which is in general system-dependent. Thus, similar to Hermitian ensembles, a comparison of the local fluctuations imposed on different spectral density backgrounds requires an "unfolding" of the levels. The latter refers to a rescaling of the eigenvalues z_k by the local mean level spacing $\Delta(z) = (R_1(z))^{-1}$ at the spectral point of interest, say z , thereby resulting in a unit local mean level density in terms of the rescaled variables; here $R_1(z)$ is the local mean level density of the eigenvalues at z before unfolding. An important technical point here is the distribution of levels on the complex plane, each level with two degree of freedom (real and imaginary parts). In order to retain the same normalization of the mean level density before and after the rescaling, it is important that both real and imaginary parts of z_k should be rescaled by $\sqrt{\Delta(z)}$. This follows from the conditions

$$\mathcal{R}_1(e) \, de \, de^* = R_1(z) \, dz \, dz^*, \quad \mathcal{R}_1(e) = 1. \quad (9)$$

The above conditions can be fulfilled e.g. by choosing

$$e_{k1} = \int dz_{k1} \sqrt{R_1(z)}, \quad e_{k2} = \int dz_{k2} \sqrt{R_1(z)}. \quad (10)$$

The spectral correlations in terms of the rescaled complex variables e_1, \dots, e_n can be given as

$$\mathcal{R}_n(e_1, \dots, e_n; Y) = \text{Lim} N \rightarrow \infty \frac{R_n(z_1, \dots, z_n; Y)}{R_1(z_1; Y) \dots R_1(z_n; Y)} \quad (11)$$

As $R_1(z_1) \approx R_1(z_2) \approx \dots R_1(z_n)$ is assumed to be locally constant, we can approximate $\Psi \equiv \prod_{k=1}^n R_1(z_k; Y) \approx (R_1(z; Y))^n$ with z as the spectral location where local density correlations are under consideration. The evolution equation for $\mathcal{R}_n(e_1, \dots, e_n; Y)$ can now be obtained by a substitution of Ψ $\mathcal{R}_n(e_1, \dots, e_n; Y)$ on both sides of eq.(5).

Subsequently the function Ψ can be taken out of the derivatives with respect to e_{ks} on the right side of eq.(5). This leads to

$$\frac{\partial \mathcal{R}_n}{\partial \Lambda_e} = \sum_{s=1}^2 \sum_{j=1}^n \frac{\partial}{\partial e_{js}} \left[\frac{\partial \mathcal{R}_n}{\partial e_{js}} - 2 \frac{\partial \ln |\Delta_n|}{\partial e_{js}} \mathcal{R}_n - 2 \int_{-\infty}^{\infty} d^2 e_{n+1} \mathcal{R}_{n+1} \frac{\partial \ln |e_j - e_{n+1}|}{\partial e_{js}} \right] \quad (12)$$

with $\Delta_n(e) \equiv \prod_{k < l}^n |e_k - e_l|$ and Λ_e is given by the relation

$$\frac{\partial \mathcal{R}_n}{\partial \Lambda_e} = \frac{1}{R_1 \Psi} \frac{\partial \Psi \mathcal{R}_n}{\partial Y} = \frac{1}{R_1} \frac{\partial \mathcal{R}_n}{\partial Y} + \frac{\mathcal{R}_n}{R_1} \frac{\partial \log \Psi}{\partial Y} \quad (13)$$

Assuming R_1 and thereby Ψ to be varying slowly with respect to Y , the term $\frac{\partial \log \Psi}{\partial Y}$ can be neglected, leading to

$$\Lambda_e = (Y - Y_0) R_1(z, Y). \quad (14)$$

As discussed in [1], however, a Y -dependence of R_1 is sensitive to the choice of the initial condition and may be too significant to be ignored; for example, for a choice of a Poisson initial condition, $R_1(z)$ varies rapidly for small $(Y - Y_0)$. For such cases, while the evolution of \mathcal{R}_n can still be described by eq.(12) but eq.(14) is no longer applicable for Λ_e . This motivates us to define Λ_e as

$$\Lambda_e = (Y - Y_0) R_{1,local}(z; Y). \quad (15)$$

where the function $R_{1,local}(z; Y)$ is determined, in principle, from eq.(13); (so named because the function has the same units as the average spectral density). Technically however this is not an easy task. Indeed, for similar studies on Hermitian ensembles, a more physically motivated, intuitive definition justified by numerical analysis has been used. As indicated by these studies, $R_{1,local}(e)$ for a d -dimensional Hermitian Hamiltonian with matrix size N depends on, besides $R_1(e)$, on the eigenfunction correlations too (at energy e) and can be formulated as (e.g. see section 6.13 of [43], [45, 48, 50, 52] and references therein)

$$R_{1,local}(e) = R_1(e) \frac{\eta(e)}{N}. \quad (16)$$

Here $\eta(e)$ is the average correlation/ localization volume at energy e and is related to the inverse participation ratio $I_2(e)$ at e : $\eta \propto (I_2)^{-1}$ for e in the bulk of the spectrum. The above definition indeed originates from the contribution of each spectral level e_n , weighted by its intensity $|U_n|^2$, to local spectral density and can be defined as $R_{1,local}(e) = \langle \sum_{n=1}^N |U_n|^2 \delta(e - e_n) \rangle$. Using $|U_n|^2 \sim \frac{\eta(e)}{N}$ then leads to the definition in eq.(16). Intuitively it seems the same definition of $R_{1,local}(e)$ can be extended to non-Hermitian case too (by replacing $|U_n|^2$ by $U_n^* V_n$). Its theoretical verification however requires a statistical study of the eigenfunction correlations too which is beyond the ambit of present study. To distinguish it from Y (the ensemble complexity parameter), hereafter Λ_e will be referred as the spectral complexity parameter.

We note that the rescaling of Y leading to Λ_e in the present case is different from the Hermitian ensembles. In the latter case, we have $\Lambda_e = (Y - Y_0) R_1^2(e; Y)$ with e as a real variable if $R_1(e; Y)$ is slowly evolving with Y (e.g. see section 6.13 of [43], [54] for Brownian ensembles), and, $\Lambda_e = (Y - Y_0) R_{1,local}^2(e)$ for cases in which $R_1(e; Y)$ varies significantly with Y even at a local mean level spacing (e.g multiparametric Gaussian ensembles discussed in [45, 48, 50, 52] and references therein). A different rescaling of Y in non-Hermitian case arises from the rescaling of both real and imaginary components of the eigenvalues.

The rescaling of Y introduces, in left side of eq.(12), an e -dependence (that was absent before) and as a consequence, the fluctuations of rescaled n^{th} order correlations retain location-dependence even after unfolding (similar to the Hermitian cases discussed in [45, 48, 51, 52]); although the latter removes the dependence on the location "z" from \mathcal{R}_n but reintroduces it through $\Lambda_e(z)$. We note that the original definition of unfolding was introduced in context of the translationally-invariant, stationary spectrum which corresponds to $\Lambda_e \rightarrow \infty$ limit of our formulation [54]). The location-dependence of \mathcal{R}_n leaves them no longer translational as well rotational invariant on the complex plane, thus making it imperative to analyze their radial and angular dependence. To analyze the latter, it is more appropriate to first rewrite eq.(5) in polar coordinates. Writing $\mathcal{R}_n(z_1, z_2, \dots, z_n)$ as $\mathcal{R}_n(r_1, \dots, r_n; \theta_1, \dots, \theta_n)$ along with $e_k = r_k e^{i\theta_k}$ and $D\Omega_{n+1} \equiv \prod_{k=n+1}^N r_k dr_k d\theta_k$, eq.(5) can be rewritten as

$$\begin{aligned} \frac{\partial \mathcal{R}_n}{\partial \Lambda_e} = & \sum_k \left(\frac{2}{r_k} \frac{\partial}{\partial r_k} + \frac{\partial^2}{\partial r_k^2} + \frac{1}{r_k^2} \frac{\partial^2}{\partial \theta_k^2} \right) \mathcal{R}_n + 2 \sum_{k,l;k \neq l} \left(\frac{\partial(C_{kl} \mathcal{R}_n)}{\partial r_k} + \frac{1}{r_k} \frac{\partial(D_{kl} \mathcal{R}_n)}{\partial \theta_k} \right) - \\ & 2 \sum_k \int dr_{n+1} d\theta_{n+1} r_{n+1} \left[\frac{\partial C_{kn+1}}{\partial r_k} + \frac{1}{r_k} \frac{\partial D_{kn+1}}{\partial \theta_k} \right] \mathcal{R}_{n+1} \end{aligned} \quad (17)$$

where $C_{km}(r_k, \theta_k, r_m, \theta_m) = \frac{r_k - r_m \cos(\theta_k - \theta_m)}{r_k^2 + r_m^2 - 2r_k r_m \cos(\theta_k - \theta_m)}$, $D_{km}(r_k, \theta_k, r_m, \theta_m) = \frac{r_m \sin(\theta_k - \theta_m)}{r_k^2 + r_m^2 - 2r_k r_m \cos(\theta_k - \theta_m)}$.

The above equation describes evolution of \mathcal{R}_n on r, θ -plane from an arbitrary initial state at $\Lambda_e = 0$ (equivalently $Y = Y_0$) to the stationary limit at $\Lambda_e = \infty$ (equivalently $Y \rightarrow \infty$). Its general solution gives in principle the radial and angular dependence of \mathcal{R}_n for arbitrary Λ_e as well as the initial conditions. In many cases, such multivariable equations can approximately be solved by a separation of variables approach but strong correlations rule out that possibility in the present case. As the theoretical determination of the solution is technically very complicated, it would be helpful to first develop some insights e.g by alternative routes. This motivates us to consider, in the next section, a numerical analysis of the spectral fluctuation measures which are not only numerically and experimentally accessible but also depend on many orders of the correlations \mathcal{R}_n .

Universality and criticality of the fluctuations: With ensemble dependence in eq.(17) appearing only through Λ_e (besides constants of evolution), \mathcal{R}_n for different ensembles are expected to undergo similar evolution in terms of Λ_e if subjected to same global constraints. The latter ensures that each ensemble can evolve from statistically same initial condition e.g an ensemble of uncorrelated eigenvalues (corresponding to Poisson statistics). We note that the set of constants of evolution i.e t_2, \dots, t_M need not be same for different ensembles; Λ_e then describes the evolution of \mathcal{R}_n for different ensembles on parallel curves in parametric space.

Following from eq.(7) and eqs.(14, 15), Λ_e is a function of many ensemble parameters and can take a same value for their different combinations i.e for different ensembles. As all statistical measures can in principle be derived from \mathcal{R}_n , their analogy across different ensembles is expected if the respective Λ_e values are equal and their initial states are statistically analogous. (For examples, the initial spectral statistics of different ensembles can belong to Poisson universality class if each consists of sparse complex matrices even if the type of their sparsity differs. This is further explained in [1] by examples). The ensemble parameters for the statistical spectral analogy of two ensembles say $\rho_1(H)$ and $\rho_2(H)$ can be obtained by invoking the condition $\Lambda_{e,\rho_1} = \Lambda_{e,\rho_2}$, with Λ_e given by eq.(15) (assuming their initial state at $\Lambda_e = 0$ is same).

Besides the spectral range, the dependence of Λ_e on the system size (i.e the matrix size N in the ensemble) also plays an important role in the above mentioned statistical dynamics. As both $(Y - Y_0)$ as well as $R_{1,local}$ can in general be N -dependent (with N as system size), we have $\Lambda_e \propto N^\alpha$ with α arbitrary and dependent on other system parameters. A variation of system conditions can cause α to vary, resulting in Λ_e varying from $0 \rightarrow \infty$. This in turn results in R_n and other spectral fluctuation measures undergo a crossover from the initial statistics to Ginibre universality class if N is finite. In the limit $N \rightarrow \infty$, a change of α may however lead to an abrupt transition from initial (for $\alpha < 0$) to Ginibre universality class (for $\alpha > 0$). An additional universality class, different from both stationary limits, could however occur if $\alpha = 0$ i.e if the underlying system conditions conspire to give rise to an N -independent, non-zero and finite Λ_e . The critical value, referred hereafter as Λ^* , indicates the existence of a non-stationary universality class in infinite size limit and characterizes the critical spectral statistics different from the two end points i.e initial and Ginibre universality class. As the existence of Λ^* depends significantly on the appropriate combination of underlying system conditions, it can differ from system to system and may not even exist for some systems (e.g. it could coalesce with either $\Lambda_e = 0$ or ∞).

We note the existence of a critical spectral statistics in a specific non-Hermitian ensemble was discussed in [19]; the criticality here was shown to be similar to a specific Hermitian case (i.e based on the exponential decay of spectral correlations beyond Thouless energy and resulting in a asymptotically linear behavior of the number variance with slope less than one). The characterization of the criticality by Λ^* mentioned above however is more general and is applicable to any non-Hermitian system described by a multiparametric Gaussian ensemble of complex matrices. This is further explained in next section by a numerical analysis of three different ensembles of complex matrices.

III. NUMERICAL ANALYSIS OF SPECTRAL FLUCTUATIONS

To achieve the objectives mentioned in section I, we numerically analyze three ensembles of complex random matrices with independent, Gaussian distributed entries with zero mean but different functional dependence of their variances. The ensemble density $\rho(H)$ in each case is given by eq.(1), with $x_{kl;s} = 0$ for all k, l and s indices but $y_{kl;s}$ varying among elements. The three ensembles considered here are same as used in [1] for numerical analysis of

ensemble averaged spectral density; the analysis of their spectral fluctuations here complements the previous study. The choice also helps to retain a knowledge of the spectral background on which the fluctuations are imposed (required for unfolding purposes).

A. Details of the ensembles

To avoid a repetition, here we mention only the details of the ensembles necessary for present analysis (with more details given in [1])

(i) Ensemble of complex matrices with constant diagonal to off-diagonal variance ratio (BE):

$$y_{kl;s} = \frac{1}{2} \left(1 + \frac{N}{b}\right)^2, \quad y_{kk;s} = \frac{1}{2}. \quad (18)$$

(ii) Ensemble of complex matrices with power law off-diagonal variance (PE):

$$y_{kl;s} = \frac{1}{2} \left(1 + \left(\frac{|k-l|}{b}\right)^2\right)^2, \quad y_{kk;s} = \frac{1}{2} \quad (19)$$

(iii) Ensemble of complex matrices with exponential off-diagonal variance (EE):

$$y_{kl;s} = \frac{1}{2} \exp\left(\frac{|k-l|^2}{b^2}\right), \quad y_{kk;s} = \frac{1}{2}. \quad (20)$$

We note that the ensemble density in eq.(18) is same as the Brownian ensemble that appears as a nonstationary perturbed state when an ensemble of diagonal matrices is perturbed by a Ginibre ensemble of complex matrices. Similar Hermitian matrix ensembles, arising as the nonstationary states due to perturbation of a diagonal ensemble by a Gaussian unitary ensemble (GUE) have also been extensively studied in past; their ensemble density is analogous to the Rosenzweig-Porter ensemble of complex Hermitian matrices too [50]. This motivates us to refer the case described in eq.(18) as a Brownian ensemble appearing between Poisson and Ginibre limit (or just BE for short). Further Hermitian ensembles, similar to eq.(19 and eq.(20) and known as power law random banded ensembles (PRBME) and exponential ensembles respectively, have also been studied in past and have been shown to be relevant for many localization to delocalization transitions of many body Hamiltonians [50]. The choice of similar ensembles in the present work makes a comparative analysis of the fluctuation measures in Hermitian and non Hermitian cases feasible, thereby providing some insights for the theoretical formulations for analogous cases, and is one of the motivations for their consideration in the present work.

As indicated above, each ensemble depends on at least two system parameters, namely, b and system size N . Contrary to BE, the off-diagonals in PE and EE depend on the distance $r = |k-l|$ from the diagonal too, with their strength decaying with r as a power-law and exponentially, respectively. This makes faraway off-diagonals relatively negligible with respect to diagonals, making a typical matrix of the ensemble effectively sparse, with sparsity in EE stronger than PE. To understand the system dependence of the spectral correlations, we exactly diagonalize thousands of matrices of each ensemble for many b values and four system sizes $N = 256, 512, 1024, 2048$.

In a previous study [1], we presented a detailed theoretical analysis of the average spectral density R_1 for the ensemble (1) and derived its formulation in terms of Y (eq.(7)) for a fixed set of global constraints. The theoretical claim was verified by a detailed numerical analysis of R_1 for BE, PE and EE; the required Y parameter in each case were obtained by the substitution of their ensemble parameters in eq.(8), and choosing $b = 1/N$ as the initial condition for each ensemble. The latter along with eq.(7) gives

$$Y - Y_0 = -2 \ln \frac{(1 + N/b)}{(1 + N^2)} \quad (BE), \quad (21)$$

$$= -\frac{2}{N^2} \sum_{r=1}^N (N-r) \ln \left(\frac{1 + r^2/b^2}{1 + N^2 r^2} \right) \quad (PE), \quad (22)$$

$$= \frac{(b^2 N^2 - 1)(N^2 - 1)}{12 b^2} \quad (EE). \quad (23)$$

As indicated by study [1], the increasing repulsion of the eigenvalues with increasing b causes eigenvalues to distribute uniformly on the complex plane with average density $R_1(r, \theta)$ approaching a constant. While the limit $b \rightarrow \infty$

corresponds to the Ginibre statistics for each ensemble, the limit $b \rightarrow 0$ the Poisson statistics. We note that $(Y - Y_0) \geq 0$ for each case, increasing from $0 \rightarrow \infty$ as b varies from $1/N \rightarrow N$. We also note, that $(Y - Y_0)$ for EE case becomes very large for all b -values above $b = 1/N$. As the average spectral density $R_1(r, \theta)$ is governed by $Y - Y_0$, this implied its rapid transition from the initial state to Ginibre limit and was numerically confirmed too in [1].

As discussed in previous section, contrary to R_1 , \mathcal{R}_n for $n > 1$, and, thereby other measures of the spectral fluctuations over the ensemble, evolve as a function of Λ_e from an arbitrary initial condition and for a fixed set of evolution constants t_2, \dots, t_M . Although not required for our fluctuation analysis, we note, for completeness sake, that (i) $M = 2N^2 - 1$ for each of the three ensembles, (ii) eq.(19) and eq.(20) can be rewritten as $y_{kl;s} = \frac{1}{2} \left(1 + \frac{t_r^2}{b^2}\right)^2$ and $y_{kl;s} = \frac{1}{2} \exp\left(\frac{t_r^2}{b^2}\right)$ with $r \equiv |k - l|$, respectively. Inverting eq.(22) and eq.(23), b in preceding relations can be replaced by $Y - Y_0$. This helps to express each $y_{kl;s}$ as a function of Y and t_r only, and thereby identification of the constants of evolution for PE and EE case as arbitrary functions of $|k - l|$. The constants for BE case however can be chosen as all equal e.g. either 1 or N . Different constants of evolution imply the evolution of three ensembles on different curves but parallel in the parametric space.

To numerically verify our theoretical claim, we need Λ_e expressed explicitly in terms of the system parameters of the three ensembles. As in [1], here again we choose $b = 1/N$ as the initial condition for each ensemble; this ensures, in large N -limit, that the initial spectral statistics in each case belongs to the Poisson universality class on complex plane. The choice also retains $Y - Y_0$ for each ensemble same as those used in [1] for the average level density analysis (given above by eq.(21, 22, 23)). But a determination of Λ_e from eq.(15) also requires a prior information about $R_{1,local}(e)$ at the spectral range e of interest; as mentioned in previous section, a complete understanding of the latter is missing so far. This handicaps us, in the present work, from theoretical prediction of Λ_e , leaving its numerical determination as the only option. As discussed below our numerical analysis suggests

$$\Lambda_e \propto (\log b - c) \quad (24)$$

with c as an ensemble dependent constant. It is worth emphasizing here that b appears differently in each ensemble and has different effect on the relative strengths of the matrix elements. Indeed a change of b in BE leaves the off-diagonals unchanged relative to each other but changes them with respect to the diagonals. On the contrary, for both PE and EE cases, the elements in any two principal off-diagonals change only relatively as b changes.

The form in eq.(24) for Λ_e can indeed be justified for BE and PE: from eq.(21) for BE, we have $Y - Y_0 \approx \ln b - c$ for $b < 1$ where $c = \ln \frac{N}{(1+N^2)}$; this would be consistent with eq.(15) if $R_{1,local}$ is constant for this case. A similar behavior for $Y - Y_0$ from eq.(22) for PE can be confirmed by the computational intelligence tools (Wolfram Alpha). Surprisingly, eq.(24) for Λ_e seems to work well for EE too (although not directly obvious from eq.(23)). Indeed, as can be seen from eq.(23), $Y - Y_0$ is almost independent of $b \sim N^\alpha$ with $\alpha \geq 0$. As showed in [1], the average level density R_1 also showed a rapid crossover from $\alpha = -1$ to $\alpha \sim 0$). But as discussed below, the local spectral correlations for EE vary smoothly in terms of the parameter $(\log b - c)$ even when $\alpha \sim 0$. Following the definition in eq.(23), the Λ_e -form in eq.(24) for EE case can then originate only from $R_{1,local}$.

B. Non-ergodicity and Non-Stationariness of the Fluctuations

The ergodicity in a random matrix ensemble implies the equivalence of the average of a measure when its behavior is considered along a single spectrum with that obtained over an ensemble for a fixed spectral point (similar to equivalence of the averages over time and the phase space of standard statistical physics). The existence of the ergodicity for the average spectral density as well as its fluctuations for a basis-invariant random matrix ensembles e.g. Gaussian orthogonal ensemble, Gaussian unitary ensemble etc was first proved in [55].

The stationarity of the spectrum however corresponds to an analogy of the local fluctuations at any two arbitrary spectral points, equivalently, translational invariance in case of the spectrum along a real line and both translational as well as rotational invariance in case of complex plane. As the statistical measure of an ergodic ensemble are translationally/ rotationally invariant along the spectrum, it is also referred as a stationary ensemble. Indeed both the ergodicity as well as stationarity of a random matrix ensemble are signatures of the underlying basis: an invariance in the latter permits the eigenfunctions to be ergodic and spectral measures to invariant along the spectrum axis.

Intuitively the average spectral density, of a non-stationary ensemble is expected to be non-ergodic: its behavior on an average over a single spectrum differs from that obtained over an ensemble while keeping the spectral point fixed [55, 56]. Indeed the theoretical study [1], supported by numerical evidence, has already indicated that the average spectral density of the ensemble (1) is in general non-ergodic. This motivates the natural query: whether the local fluctuations imposed on a non-ergodic background will retain non-ergodicity even after unfolding? As discussed in [43, 49, 56, 57], the conditions for ergodicity differ from one measure to another and its lack for average spectral

density need not hinder its existence for the spectral fluctuations. We note that, in case of the latter, ergodicity can at best be defined locally: it exists if the local fluctuations *in a range Δz around an arbitrary spectral point "z" for a single matrix* are analogous to those *over an ensemble at the point "z"*. We refer such a spectrum as "locally ergodic" and emphasize that it differs from the non-stationarity of the fluctuations.

Besides improving statistical accuracy and thereby enabling a meaningful comparison of the local fluctuations, the information about the local ergodicity is needed, in the present context, for another reason too. In case of a stationary ensemble, the local fluctuations of the spectral density depend only on its spectral average, equivalently, its ensemble average due to ergodicity; the unfolding maps the latter to a constant and thereby mapping the local fluctuations on a constant background. But as indicated by eq.(12), the local fluctuations in a non-stationary ensemble depend on both $R_{1,local}(z)$ as well as $Y - Y_0$ (from the definition of Λ_e) and while the unfolding removes their explicit dependence on the location z on the complex plane, the latter is still retained, implicitly, through Λ_e . Indeed this is the ensemble's non-stationarity manifesting through non-stationarity of the local fluctuations even after unfolding. As a consequence, a spectral averaging e.g. of the spacings over a finite spectral width, say $z - \delta z, z + \delta z$, can lead to mixing of statistics with different Λ_e unless $\delta(z)$ is very small or the local average density is almost constant (thereby leaving Λ_e almost constant). While this can be avoided by considering just the ensemble averaging i.e by taking a single (or two) unfolded spacing S_k at spectral point z from a matrix and averaging over all the matrices in the ensemble, this in turn requires a large ensemble size for accuracy purposes and therefore huge computational time.

The existence of local ergodicity in the spectrum helps in the above context: the unfolded spacing averages over an ensemble at a spectral point, say "z" can be approximated by the double averages i.e those over an ensemble as well as in an optimized spectral range around "z" (small enough to keep Λ_e almost constant). For example, in the spectral regions where $R_1(z)$ varies very slowly, it is possible to choose an optimized range in the neighbourhood of z , sufficiently large for good statistics but keeping a mixing of different statistics at minimum. (Note this is usually not the case for the regions e.g. edge with sharp change of $\Delta(z) = (R_1(z))^{-1}$; the latter leads to a rapidly changing Λ_e and it is numerically difficult to consider a spectral range with an appropriate number of levels without mixing of different statistics).

As shown in figures 1-3 of [1], the eigenvalues for each of the three ensembles are distributed over a complex plane with a non-ergodic, Y -dependent density and, as a consequence, their rescaled (unfolded) spacings can vary (i) from one spectral range to another at a fixed Λ_e , or (ii) with Λ_e at a fixed spectral range. (The corresponding behaviour for Hermitian ensembles is discussed in detail e.g. in [51]). The nearest neighbour spacing distribution (NNSD) $P_e(S, \Lambda_e, e)$ for the rescaled eigenvalues therefore depends on the variables S, Λ_e as well as e , with S as a nearest neighbour spacing in the neighbourhood of a point e on the spectral plane with Λ_e as the ensemble complexity parameter (definition of P_e given in *appendix B*). Here the unfolding of the spacing is achieved by rescaling it by the local mean spectral density numerically defined as [15–17]

$$R_{1,unf} = \frac{n}{\pi d_{n,k}^2} \quad (25)$$

where n is an optimized number of the eigenvalues, sufficiently larger than unity but small compared to the matrix size N and $d_{n,k} \equiv |z_{n+k} - z_k|$ is the n^{th} nearest neighbour distance from z_k (before unfolding). The rescaled spacing are then defined as $S_k = d_{1,k} \sqrt{R_{1,unf}}$. (We note that the function in eq.(25) corresponds to an unfolding of each spectrum locally and is used in many previous studies [15–17]. Alternatively, it can also be done by the approximate $R_1(r, \theta)$ formulation derived in our previous work [1] but the final results remain affected).

To seek presence/ absence of the local spectral ergodicity, we consider two different averaging approaches for each of the three ensembles. The first averaging route, referred as the *ensemble averaging*, is as follows: We recall that, each eigenvalue on the complex plane has more than two neighbors; (this is contrary to the Hermitian case in which the eigenvalues are confined on real lines and each eigenvalue has two nearest neighbors). We first choose one of the eigenvalues at $e \sim 0$ from a matrix, choose its spacing with nearest neighbor. As the exact eigenvalue at $e \sim 0$ or its nearest neighbor spacing indeed need not be same for different matrices, we study the distribution of such spacings over an ensemble of 2500 matrices; thus the total number of eigenvalues used for the analysis are 2500. (This corresponds to using the definition $P(S, \Lambda_e) = \langle \sum_k \delta(S - S_k) \rangle$ with $\langle \rangle$ as the ensemble average). The second route, based on both spectral as well as ensemble averaging and referred here as *spectral-ensemble averaging* is as follows: we consider 10% spacings around $e = 0$ for each matrix in the ensemble, obtain their distribution for the matrix and then average it over the ensemble; (for the matrix size $N = 1024$, this corresponds to ~ 100 spacing taken from a single matrix with ensemble size $M = 25$). (This corresponds to using the definition $P(S, \Lambda_e) = \langle \sum_k \delta(S - S_k) \rangle$ with \bar{x} as the spectral average). The number of levels used in each case are kept same, to avoid non-physical deviations arising from e.g. finite size sample errors.

Figure 1 displays a comparison of the $P(S, \Lambda_e)$, obtained by the two averaging approaches, in the neighborhood of the region $e \sim 0$ for three b -values (equivalently for three Λ_e) for each of the three ensembles. While a slight deviation between the two averagings is clearly visible from figure 1 for each of the three ensembles for $b \ll N$, it survives,

albeit rather weakly, even for the Ginibre limit ($b = N$ case) of each ensemble too. Theoretically however the Ginibre ensemble as well as its local fluctuations are expected to be stationary. This suggests the deviation to be an artefact of the finite sample errors. Indeed the two types of averaging are almost in agreement for each ensemble, thereby suggesting the local ergodicity of the fluctuations. But the latter does not imply stationarity of the spectrum. This can further be illustrated by a consideration of the Ginibre ensemble directly; as the latter's spectrum is stationary, the distribution of $P(S, \infty)$ is expected to be independent of the location "e" and is indeed confirmed in figure 2. In contrast, as indicated by our numerics, the deviation for BE, PE and EE are sensitive to the spectral location of the single spacing thus indicating non-stationarity of the spectrum (corresponding figure not included here). Further the analogy of the two averages for the Ginibre ensemble for 1st spacing is visibly better than PE and EE cases for $b = N$; this suggests the fluctuations reaching an almost Ginibre limit, but not exactly, for them.

C. Lack of Sensitivity to Multiple System Parameters: emergence of Complexity Parameter

As discussed in section II, the fluctuations are governed by a single functional Λ_e describing a collective influence of the system conditions and not their individual details. Λ_e can however be changed by changing Y i.e by changing the system conditions. Thus the unfolded correlations can change even at a given spectral point "e" if the system parameters and thereby ensemble parameters are varied. Based on our theoretical prediction, a variation of the ensemble parameters should lead to an analogous crossover in a spectral fluctuation measure for different ensembles if they share statistically same initial and final endpoints. To verify the above, here we statistically analyze each ensemble by varying the parameter b and thereby $Y - Y_0$. As the latter changes the average mean level density R_1 too, this affects Λ_e both explicitly as well as through R_1 .

Contrary to a stationary spectrum, the local correlations in our case are not translational or rotational invariant i.e vary on the complex spectral plane from one point to another for a fixed set of system conditions i.e for a fixed Y . An unfolding of the levels maps them, locally, to a constant background. As this renders the fluctuations locally ergodic, one can consider levels within an optimized spectral range without mixing the statistics. But as the fluctuations of the unfolded eigenvalues are nonstationary (governed by Λ_e that varies along the spectrum), it is necessary to choose an optimize range Δe that contains sufficient number of eigenvalues to give good statistics but all with almost same Λ_e . We analyze 10% of the total eigenvalues taken from a range Δe centred at $e \sim 0$ for $N = 1024$ and for an ensemble size of 2500 matrices; this gives total $\sim 10^5$ eigenvalues for the analysis for each ensemble which are unfolded by $R_{1,unf}$ given by eq.(25).

As the non-stationarity of the spectrum renders a definition of the long range spectral measure not very clear (unfolding not leaving them locally stationary), here we consider two fluctuation measures, both indicators of short range spectral behavior.

Spacing Distribution: While no theoretical formulation is currently available for the $P_e(S, \Lambda_e)$ intermediate between Poisson and Ginibre limit, its approximation by R_2 (appendix B) suggest, along with eq.(17), a smooth crossover governed by Λ_e . Thus the form of $P_e(S, \Lambda_e)$ is expected to be intermediate between Poisson ($\Lambda_e = 0$, eq.(B2)) and Ginibre universality class ($\Lambda_e = \infty$, eq.(B3)) if Λ_e is finite and non-zero. Figure 3 displays the $P_e(S, \Lambda_e)$ behavior for each of the three ensembles for many b -values, equivalently many Λ_e values obtained from eq.(24). Here again, the spacings considered for the analysis consist of only 10% eigenvalues from the neighborhood of $e \sim 0$ for a fixed matrix size $N = 1024$ and for an ensemble of 2500 complex matrices. As clear from the figure, the statistics undergoes a crossover from Poisson to Ginibre statistics as Λ_e varies. We recall that the off-diagonal variances in PE and EE depend on additional system conditions; this manifests through the difference of their decay types, mentioned in the beginning of section III.A) and thereby $Y - Y_0$. Although the latter has different mathematical form for the three ensembles, and, its variation effectively implies variation of more than one system parameter for PE and EE (as clear from eq.(21, 22, 23)), $P_e(S, \Lambda_e)$ seems to evolve between two stationary limits in an analogous way for the three ensemble. (A slight deviation of the peak towards left for BE cases seems to be an artefact of unfolding issues with local mean level density changing more rapidly than PE and EE).

The numerical results shown in figure 3 encourage us to conjecture a form of P_e , based on a single parametric interpolation between two stationary limits i.e Poisson at $\Lambda_e = 0$ and Ginibre at $\Lambda_e = \infty$,

$$P(S, \Lambda_e) = A S^B e^{-C S^2} \quad (26)$$

subjected to the normalization condition $\int_0^\infty P(S) dS = 1$ and unit mean level spacing condition $\int_0^\infty S P(S) dS = 1$. Here $B = 1$ corresponds to Poisson limit (on a plane) and $B = 3$ gives the approximate Ginibre limit [16, 43]. To justify the single parameter formulation, it is desirable to express the fitted parameters A, B, C as as functions of Λ_e . As given in table 1, these parameters can indeed be recast as functions of Λ_e .

We note, that previous numerical studies of $P(S; \infty)$ for non-Hermitian case (i.e Ginibre ensemble) indicate an important difference from the Hermitian one (i.e Gaussian unitary ensemble): although, in the latter case, the Wigner

TABLE I. The table gives the fitted parameters A, B, C for eq.(26 used in figure 4 for BE, PE and EE respectively. Based on the numerics, the fitted parameters can be recast in the suggestive forms as a function of Λ_e ; this is given in the second row for each case The second row for each case gives the suggested Λ_e dependence of A, B, C .

Case	Λ_e	A	B	C
BE	$\log b + 3.79$	$6.78(\log b + 3.15),$ $\sim 6.78\Lambda_e,$	$2.1(\log b + 3.79) - 0.31,$ $\sim 2.1\Lambda_e,$	$0.92 \log b + 3.79;$ $\sim \Lambda_e$
PE	$\log b + 1.48$	$7.39(\log b + 1.03),$ $\sim 7.39\Lambda_e,$	$3.27(\log b + 1.2),$ $\sim 3.27\Lambda_e,$	$1.43(\log b + 1.48)$ $\sim 1.43\Lambda_e$
EE	$\log b - 1.17$	$6.01(\log b - 1.88),$ $\sim 6.01\Lambda_e,$	$2.06(\log b - 1.17) - 0.46,$ $\sim 2.06\Lambda_e,$	$\log b - 1.17 ,$ Λ_e

surmise for $P(S)$ is exact for $N = 2$ case only, it has been shown to be well-applicable for large N case too. The large N limit of $P(S)$ for Ginibre ensemble however deviates significantly from the $N = 2$ result [16]; (see eq.(B3) of appendix B); this suggests emergence of new spectral correlations on the plane as N increases. As displayed in figure 4, the good agreement of our numerical results with eq.(26) indeed supports the above conjecture. The numerically fitted values for the parameters A, B, C and their suggested Λ_e dependence for each ensemble is given in table 1. Here again the definition $\Lambda_e = \log b - C$ as the crossover parameter seemingly apply quite well.

Spacing Ratio Distribution:

As briefly discussed in appendix C, the unfolding related technical issues and errors can be avoided by the consideration of a dimensionless short range fluctuation measure. i.e the nearest neighbour spacing ratio, previously introduced for the real eigenvalues of Hermitian ensemble [59, 60]. With eigenvalues of a complex matrices distributed on a complex plane, a generalization of the spacing ratio measure, referred as the distribution of the complex spacing ratios, was later introduced in [15] for non-Hermitian ensembles.

A complex spacing ratio Z_k is defined as the ratio of the nearest neighbour spacing and next nearest neighbour spacing of a given eigenvalue z_k on the complex plane

$$Z_k = \frac{z_k^{NN} - z_k}{z_k^{NNN} - z_k}. \quad (27)$$

with $0 \leq Z_k \leq 1$, z_k^{NN} and z_k^{NNN} as the nearest neighbor and next nearest neighbor eigenvalue of z_k . The probability density $P_z(Z)$ of finding a spacing ratio Z over an ensemble for a specific spectral range is then free of unfolding issues and contains information not only about the radial correlations but the angular ones too [15]. The latter can also be seen directly from the marginal distributions of the radial and angular parts of the spacing ratio; writing $Z = r e^{i\theta}$, we have

$$\rho_r(r) \equiv \langle P_z(Z) \rangle_\theta = \int d\theta r P_z(Z), \quad (28)$$

$$\rho_\theta(\theta) \equiv \langle P_z(Z) \rangle_r = \int dr r P_z(Z). \quad (29)$$

For uncorrelated eigenvalues distributed on a complex plane, the spacing ratios are isotropic and consequently [15]

$$\rho_{r,poi}(r) \propto r \Theta(1 - r) \quad (30)$$

with subscript "poi" as the reference to Poisson statistics. No closed form expression for large N is however known for Ginibre ensemble of complex matrices (referred as GinUE in [15]). Although an exact result is obtained for $N = 3$ in [15] but, contrary to Hermitian case, it is not a good approximation in large N limit; (we recall that exact for $N = 2$ for Hermitian matrices well approximates large N behavior too). As discussed in [15], the leading order expansion in powers of r in large N -limit yields $\rho_{r,gin}(r) \propto r^3$ (with subscript "gin" as the reference to Ginibre statistics) valid only for spectral range around $r = 0$. In the regime intermediate to Poisson and Ginibre ensemble, however, no theoretical results are currently available for either $P_z(Z)$, $\rho_r(r)$ or $\rho_\theta(\theta)$.

Figure 5 displays the behavior for $\rho_r(r)$ and $\rho_\theta(\theta)$ for the three ensembles in the bulk of the spectrum near $e \sim 0$ for many b -values. To numerically calculate $\rho_r(r)$, we again consider 10% spacing-ratios around $e = 0$ for each matrix in the ensemble, obtain the distribution of its radial part for the matrix and then average it over the ensemble; (for the matrix size $N = 1024$, this corresponds to ~ 100 spacing taken from a single matrix with ensemble size 2500).

Similarly $\rho_\theta(\theta)$ is obtained by considering the distribution of the angular part for the spacing ratios for each matrix and subsequently averaging it over the ensemble. Besides reconfirming the information contained in figure 3, i.e a smooth crossover from Poisson to Ginibre with increasing b and thereby Λ_e for each ensemble, the left panel of the figure 5 also indicates

- (i) an almost power law variation of $\rho_r(r)$ with r for a fixed Λ_e ,
- (ii) an increasing b resulting in decrease of $\rho_r(r)$ for $r < 0.5$ but its increases for $r > 0.5$,
- (iii) while the curves for intermediate b values lie between Poisson and Ginibre limit in both regions $r < 0.5$ and $r > 0.5$, they seem to converge in the neighborhood of $r \sim 0.5$. More clearly, as $\rho(r)$ at $r \approx 0.5$ is almost same irrespective of b , equivalently Λ_e , this indicates Λ_e -insensitivity of $\rho(r)$ at $r \approx 0.5$ and suggest, in limit $N \rightarrow \infty$, an existence of the critical point of statistics at $r \sim 0.5$. We note, from eq.(27), this corresponds to a specific relation between two nearest neighbors of a given eigenvalue.

As displayed in the right panel of figure 5, $\rho(\theta)$ drops rapidly near $\theta = 0$ as b and thereby Λ_e increases; clearly the drop occurs due to increasing level repulsion with Λ_e . But, in comparison to $\rho(r)$, the variation in $\rho(\theta)$ with Λ_e is more conspicuous; this indicates the important role played by angular correlations in the statistics. We also note that the case $\Lambda_e = 0$ is indeed almost constant and is therefore in agreement with theoretical prediction for Poisson universality class (on the complex plane).

D. Universality and Criticality in Spectral Statistics

Based on eq.(5), our theoretical claim is the following: different ensembles subjected to same global constraints are expected not only to undergo similar evolution of the spectral statistics but also to display same statistics if their Λ_e values are same. It will be instructive to verify the claim for BE, PE and EE where, due to different variance structures, it is not at all obvious as to why their statistics be analogous for some specific set of system parameters. The Λ_e values for BE, PE and EE, where their statistics are predicted to be analogous, can in principle be determined by invoking the condition $\Lambda_{e,BE} = \Lambda_{e,PE} = \Lambda_{e,EE}$, with Λ_e given by eq.(15). Due to a current lack of understanding about $R_{1,local}(e)$, however, here we consider a more general route: instead of comparison at a single Λ_e value, we compare the local fluctuations for the three ensembles for full crossover, from $b = 1/N \rightarrow b = N$, as a function of Λ_e defined in eq.(24); an agreement would indicate that the analogy is not just an accidental coincidence for some b value and indeed exists with Λ_e defined by eq.(24).

The parametric evolution of the spectral fluctuations between two stationary limits can be best studied by analyzing an average measure. A traditionally used measure in this context is the cumulative nearest neighbour distribution $I(x, e, \Lambda_e) = \int_0^x P_e(S, e; \Lambda_e) dS$ with x as an arbitrary point. Alternatively, a related measure, particularly useful for the phase transition studies, is the relative behavior of the tail of the nearest-neighbour spacing distribution P_e , defined as

$$\gamma(x; e, \Lambda_e) = \frac{I(x, e; \Lambda_e) - I(x, e; \infty)}{I(x, e; 0) - I(x, e; \infty)} \quad (31)$$

We choose x as one of the two crossing points, referred as x_1, x_2 , of $P_e(S, e; \infty) = P_{gin}(S)$ and $P_e(S, e; 0) = P_{poi}(S)$ (here the subscripts *gin* and *poi* refer to the Ginibre and Poisson cases respectively): $x_1 = 0.656978$ and $x_2 = 1.446259$. As obvious, $\gamma = 0$ and 1 for the Ginibre and Poisson limit respectively and a fractional value of γ indicates the probability of small-spacings, and thereby short range correlations, different from the two limits. In limit $N \rightarrow \infty$, a γ value different from the two end points is an indicator of a new universality class of the spectral statistics and therefore its critical point.

For comparison, we consider the γ behavior with respect to a parameter, namely, $\tau \equiv \log(b) - C$ with $C = 0, 1.8, 4.6$ for BE, PE and EE respectively; we note that, from eq.(24), τ is directly related to Λ_e . Figure 6 shows a comparison of the τ -variation of $\gamma_1 \equiv \gamma(x_1, e; \tau)$ and $\gamma_2 \equiv \gamma(x_2, e; \tau)$, in the neighborhood of the spectral point $e \sim 0$, for two x -values and three ensembles for a fixed $N = 1024$. The collapse of $\gamma(x; \tau)$ behavior for each of the three ensemble onto a single curve confirms our theoretical claim regarding a single parameter based universality of the local fluctuations. Figure 6 also shows a comparison of the variation of (i) radial part $\langle r \rangle$, and (ii) angular part $-\langle \cos(\theta) \rangle$ of the mean level spacing ratio (with r_k, θ_k referring to radial and angle part of the average spacing ratio Z_k) for three ensembles. Here the averages $\langle r \rangle$ as well as $-\langle \cos(\theta) \rangle$ are numerically obtained by the average of r_k and $-\cos \theta_k$ over an optimized energy range (10% eigenvalues around $e \sim 0$) as well as the ensemble of 2500 matrices. With N large, this permits us to consider a large number of eigenvalues for the level statistics while ensuring that they belong to same Λ_e . The good agreement for the three ensembles, of the two measures for entire crossover, once again confirms our theoretical claim regarding the single parameter dependence of the fluctuations. We note that while γ_1, γ_2 are cumulative spacing distributions, $\langle r \rangle$ and $-\langle \cos(\theta) \rangle$ are related to a dimensionless measure i.e the spacing ratio. Further as the collapse

of each fluctuation measure for the three ensembles occurs when plotted with respect to $\tau = \log(b) - C$; this again strongly suggests $\Lambda_e \propto \tau$.

The illustrations in figure 6 suggest another important aspect of the fluctuations, namely, the existence of a critical statistics: as $\log(b)$ increases, $\gamma_1, \gamma_2, \langle r \rangle$ and $-\langle \cos \theta \rangle$ undergo a rapid transition from Ginibre ($\gamma_{1,2} = 1$) to Poisson limit ($\gamma_{1,2} = 0$); this in turn suggests the existence of a critical statistics near $\log(b) - c \approx -2.5$. Indeed it is worth noting while the three ensembles have different variance structures of the matrix elements, the point of inflection seems to be same in terms of the parameter $\log b - C$.

As mentioned in previous section, the spectral statistics of a non-stationary ensemble approaches, in limit $N \rightarrow \infty$, one of three universality classes i.e either to two end points or the critical statistics. The latter is, by definition, size-independent and is characterized by a size-independent Λ_e . We note that a similar criticality of the Brownian ensemble has already been reported for Hermitian cases [50]. To confirm the existence of a critical point, it is therefore necessary to analyze the size-dependence of the spectral measures at the critical b -values (those resulting in size-independent Λ_e). We again numerically analyze $P(S, e; \Lambda_e)$ for the BE case, with a b -value arbitrarily chosen intermediate between Poisson and Ginibre limits, and, for 10% eigenvalues lying in the neighborhood of $e \sim 0$ and for the matrix sizes $N = 256, 512, 1024, 2048$ with ensemble size as 10000, 5000, 2500, 1250 respectively; this gives the total number of eigenvalues used for the analysis as $\sim 2.5 \times 10^5$ for each case. As displayed in figure 7, $P(S, e; \Lambda_e)$ behavior seems to be almost insensitive to the system size N . This motivates us to consider the measures $\gamma_1, \gamma_2, \langle r \rangle, -\langle \cos \theta \rangle$ for BE for many b -and N -values (again using the same spectral sample as mentioned above). As displayed in figure 6, the measures turn out to be size-independent for almost entire b -range, thus indicating the statistics as critical for arbitrary b value, and thereby implying ensemble in eq.(18) itself to be critical. (The existence of similar infinite family of critical ensembles for Hermitian matrices has already been discussed e.g. in [48, 50, 53]). As the figure indicates, the $b = 1/N$ and $b = N$ cases correspond to $\langle r \rangle = 0.67$ and $\langle r \rangle = 0.75$ respectively. As indicated by $P(S)$ -study, all three ensembles approach Poisson limit for $b = 1/N$ and Ginibre limit for $b = N$. We note that the measures $\langle r \rangle$ and $-\langle \cos \theta \rangle$ were also used in [17] for phase transition studies in a two coupled non-Hermitian Hatano-Nelson chains of interacting fermions in the presence of a random potential; the study indicated $\langle r \rangle = 0.5$ as the Poisson limit.

Figures 8 and 9 display the corresponding behavior of the above measures for PE and EE case too. As in the BE case, here again the collapse of the curves for almost entire b -range and different N values, for each of the measure, namely, $P(S, \Lambda_e), \gamma_1, \gamma_2, \langle r \rangle, \langle \cos \theta \rangle$, indicates the criticality of PE and EE with their distribution parameters given by eq.(19) and eq.(20); (the Hermitian ensembles with similar variance structures are also known to form an infinity family of critical ensembles [48, 50, 53]). The results in figures 7-9 also reconfirm $\log b$ as the parameter governing the spectral statistics; this in turn strongly suggests Λ_e as a function of $\log b - C$. A comparison with non-zero C values in figure 6 thus suggest C as a ensemble specific constant, independent of size N .

An important aspect of complexity parameter formulation for both Hermitian as well non-Hermitian ensembles is its role as the criteria to determine the critical spectral statistics. The present analysis confirms the validity of the criteria for complex matrix ensembles with critical spectral statistics appearing between Poisson and Ginibre universality classes: it occurs at the system conditions that keep rescaled complexity parameter Λ size-independent. As this occurs for a specific combinations of system parameters, its existence is not always guaranteed for all ensemble types.

The existence of critical spectral statistics for a specific variance structure of the matrix elements irrespective of the global constraints e.g. presence or absence of the Hermiticity indicates a hidden critical structure among complex systems: clearly a Hermitian ensemble perturbed by a non-Hermitian one with a critical variance structure of the matrix elements (i.e of type given by eqs.(18, 19, 20) is expected to be critical too in its spectral statistics. As the latter is in turn known to be related to multifractality of the eigenfunctions (for Hermitian case), this reflects a special kind of quantum correlations hidden underneath the quantum dynamics of these systems.

IV. CONCLUSION

We numerically analyze various physical aspects e.g. ergodicity vs non-ergodicity, universality and criticality of the local spectral fluctuations for non-stationary complex random matrix ensembles representing non-Hermitian many body/ disordered Hamiltonians with changing system conditions and away from equilibrium. Based on analysis of three prototypical, basis-dependent ensembles, subjected to same global constraints but with their variance structure representing three different types of quantum correlations in underlying basis space, our results clearly reveal non-ergodic, non-stationary as well as the critical aspects of the spectral correlations. This information is relevant not only for fundamental interests in such ensembles but also in context of quantum information, neural networks as well as the non-Hermitian many body localization e.g. whether or not a non-Hermitian system can achieve thermalization?

The most important insight provided by our numerical analysis is following: notwithstanding different variance structures, we find that the spectral statistics for each ensemble undergoes an analogous crossover from Poisson to

Ginibre universality class in terms of a single parameter Λ_e and also numerically identify the latter. This indicates a universality in bulk spectral statistics underlying in non-equilibrium regime of non-Hermitian systems and is consistent with theoretical claims based on complexity parametric approach reported in [1, 2]. A lack of theoretical formulations of measures handicaps us from a comparison of our numerical results with theory but indirect verification is given by analogy of evolving statistics, between two stationary limits, for each ensemble in terms of Λ_e .

For a deeper insight in the complexity parameter based formulation of the complex systems, it is relevant to compare present results with those already known in the domain of conservative systems. In case of the latter undergoing localized to delocalized transition with changing system conditions e.g. disorder or many body interactions, the Hermitian ensembles representing them undergo a crossover/abrupt transition of spectral statistics from Poisson to one of the ten stationary universality classes. As confirmed by previous studies, the transition can be well-described by Λ_e , the spectral complexity parameter [45, 50]. Similar studies on Hermitian ensembles with additional constraints e.g. positive definiteness or column constraint have also indicated the existence of non-equilibrium universality classes of spectral statistics, characterized by Λ_e [46, 51]. While the basic idea remains same as in Hermitian case, the nature of the universality classes in non-Hermitian cases is expected to be different. While we do have a clear understanding of the ensemble complexity parameter Y for non-Hermitian cases, a theoretical formulation of Λ_e is still missing. As in the Hermitian case, its technical definition is again expected to be dependent on eigenfunction correlation and therefore requires a detailed analysis of the latter.

Besides questions of eigenfunction fluctuations, our study gives rise to many other queries e.g. can the complexity parameter formulation be extended to non-Gaussian ensembles as well as to structured ensembles with correlated matrix elements? The information is relevant in order to model more generalized class of non-Hermitian systems e.g. neural networks where existence of additional matrix constraints can lead to many types of matrix elements correlations. For application to many body non-Hermitian systems it is relevant to analyze as to how the behavior of spectral correlations in the edge differ from the bulk? Another very important question, especially in context of topological materials is the existence of exceptional points and their effect on the statistical behavior of the left and right eigenfunctions. The information is needed to understand e.g. the non-Hermitian skin effect [58] and the absence of conventional bulk-boundary correspondence in topological and localization transitions in non-Hermitian systems and also for applications to biological neural networks. We intend to answer some of the above queries in near future.

-
- [1] M. G. Ansari and P. Shukla, *J. Phys. A: Math. & Theo. (IOP)*, 57, 095005, (2024).
 - [2] P. Shukla, *Phys. Rev. Lett.* 87, 19, 194102, (2001).
 - [3] M. V. Berry, *Czechoslovak J.Phys.* 54, 1039, (2004).
 - [4] F.Haake et al., *Z.Phys. B*, 88, 359, (1992).
 - [5] T. Guhr, G.A. Muller-Groeling and H.A. Weidenmuller, *Phys.Rep.* 299, 189, (1998).
 - [6] M.L. Mehta, *Random Matrices* (Academic Press, Boston, 1991).
 - [7] Y. Ashida, Z. Gong, and M. Ueda, *Advances in Physics* 69, 249 (2020).
 - [8] Z. Gong, Y. Ashida, K. Kawabata, K. Takasan, S. Hi-gashikawa, and M. Ueda, *Phys. Rev. X*8, 031079 (2018).
 - [9] A. amir, N. Hatano and D. R. Nelson, *Phys. Rev. E* 93, 042310, (2016).
 - [10] Y. Ahmadian, F. Mumarola and K. D. Miller, *Phys. Rev. E* 91, 012820, (2015).
 - [11] N.Moiseyev, *Non-Hermitian Quantum Mechanics* (Cambridge University Press, 2011).
 - [12] Y. C. Hu and T. L. Hughes, *Phys. Rev. B*84, 153101 (2011).
 - [13] H. Schomerus, *Opt. Lett.*38, 1912 (2013).
 - [14] K. Ranjan and L. F. Abbott, *Phys. Rev. Lett.*, 97, 188104, (2006).
 - [15] L. Sa, P. Ribciro and T. Prosen, *Phys. Rev. X*, 10, 021019, (2020).
 - [16] R. Hamazaki, K. Kawabata, N. Kura and M. Ueda, *Phys. Rev. Res.*, 2, 023286, (2020).
 - [17] K. Suthar, Y-C Wang, Y-P Huang, H.H.Jens and J-H You, *Phys. Rev. B* 106, 064208 (2022).
 - [18] O. Bohigas and M. P. Pato, *J. Phys. A: Math. Theor.* 46, 115001, (2013).
 - [19] A. M. Garcia-Garcia, S. M. Nishigaki and J.J.M. Verbaarschot, *Phys. Rev. E* 66, 016132, (2002).
 - [20] G.De Tomasi and I. Khaymovich, *Phys. Rev. B*, 106, 094204 (2022).
 - [21] J. Feinberg and A. Zee, *Phys. Rev. E*59, 6433 (1999).
 - [22] L. G. Molinari, *Journal of Physics A: Mathematical and Theoretical* 42, 265204 (2009).
 - [23] Y. Huang and B. I. Shklovskii, *Phys. Rev. B* 101, 014204 (2020).
 - [24] G. L. Celardo, M. Angeli, and R. Kaiser, arXiv preprint arXiv:1702.04506 (2017).
 - [25] F. Cottier, A. Cipris, R. Bachelard, and R. Kaiser, *Phys. Rev. Lett.*123, 083401 (2019).
 - [26] C. E. Maximo, N. A. Moreira, R. Kaiser, and R. Bachelard, *Phys. Rev. A*100, 063845 (2019).
 - [27] C.M. Bender, N. Hassanpour, D.W.Hook, S.P.Klevansky, C. Sunderhauf and Z. Wen, *Phys. Rev. A* 95, (2017).
 - [28] C.M. Bender and S. Boettcher, *Phys. Rev. Lett.* 80, 5243, (1998).
 - [29] C.M. Bender, D.C. Brody and H.F.Jones, *Phys. Rev. Lett.* 89, (2002).
 - [30] J. Feinberg and A.Zee, *Phys. Rev. E* 59, 6433, (1999)

- [31] Y.V.Fyodorov and H.-J. Sommers, J. Math. Physics (N.Y.), 38, 1918, (1997).
 [32] H.J.Sommers et al., Phys. Rev. Lett., 60, 1895 (1988).
 [33] N.Hatano and D.R.Nelson, Phys. Rev. Lett. 77, 570 (1996).
 [34] K.B.Efetov, Phys Rev. B 56, 9630 (1997).
 [35] I.Y.Glodsheid and B.A.Khoruzhenko, Phys. Rev. Lett., 80,2897 (1998).
 [36] C.Mudry, B.D.Simons and A.Altland, Phys. Rev. Lett., 80,4257 (1998).
 [37] J.T.Chalker and Z.J.Wang, Phys. Rev. Lett. 79, 1797, (1997).
 [38] D.R.Nelson and N.M.Shnerb, cond-mat/9708071.
 [39] J.T.Chalker and B.Mehlig, Phys. Rev. Lett. 81, 3367, (1998).
 [40] Y.V.Fyodorov, B.A.Khoruzhenko and H.-J. Sommers, Phys. Rev. Lett., 79, 557, (1997).
 [41] Nils Lehmann and H-j Sommers, Phys. Rev. Lett. 67, 941, (1991).
 [42] Y.V.Fyodorov and B.A.Khoruzhenko, Ann. Inst. Henri Poincare (Physique Theorique), 68, 449, (1998).
 [43] F. Haake, Quantum Signatures of Chaos (Springer-Verlag, Berlin, 1991).
 [44] A.Pandey and P.Shukla, J. Phys. A: Math. Gen. , 24, 3907, (1991).
 [45] P.Shukla, Phys. Rev. E 62, 2098, (2000); J. Phys. A 41, 304023 (2008); Phys. Rev. E 71, 026266 (2005); Phys. Rev. E 75, 051113, (2007); J. Phys. A: Math. Theor 50, 435003 (2017); Phys. Rev. B, 98, 054206 (2018).
 [46] M. V. Berry and P.Shukla, J. Phys. A 42, 485102 (2009).
 [47] R. Dutta and P. Shukla,ibid. 76, 051124 (2007); 78, 031115 (2008).
 [48] Pragya Shukla, J. Phys. A: Math. Theor. 54 275001, (2021).
 [49] S. Sadhukhan and P. Shukla, Phys. Rev. E 96, 012109 (2017).
 [50] P. Shukla, New J. Phys. 18, 021004 (2016). .
 [51] T. Mondal and P.Shukla, Phys Rev. E 102, 032131 (2020)
 [52] P. shukla, Int. Jou. of Mod.Phys B (WSPC), 26, 12300008, (2012).
 [53] P. Shukla, J. Phys.: Condens. Matter 17, 1653 (2005).
 [54] J.B. French, V.K.B. Kota, A. Pandey and S. Tomsovic, Annals of Physics, 181, 198 (1988).
 [55] A. Pandey, Ann. Phys. 119, 170, (1979).
 [56] O. Bohigas and M. J. Giannoni, Ann. Phys. 89 422 (1975).
 [57] T A Brody, J Flores, J B French, P A Mello, A Pandey and S S M Wong Rev. Mod. Phys. 53 385 (1981).
 [58] N. Okuma, K. Kawabata, K. Shiozaki, and M. Sato, Phys.Rev. Lett.124, 086801 (2020).
 [59] A Pal and D A Huse, Phys. Rev. B 82, 174411 (2010); V Oganessian, A Pal and D A Huse, Phys. Rev. B 80, 115104 (2009).
 [60] Y Atas, E Bogomolny, O Giraud and G Roux, Phys. Rev. Lett. 110, 084101 (2013).

Appendix A: Complexity paramter formulation of spectral correlations

As discussed in [1, 2], a change in system conditions can affect the matrix elements H_{kl} as well as the ensemble parameters in eq.(1), resulting in mutiparametric evolution of $\tilde{\rho}(H)$ in matrix space. The transformation of parameters, with help of its Gaussian form further leads to single parametric formulation of the evolution equation for $\tilde{\rho}(H)$ with a constant diffusion and finite drift [1, 2],

$$\frac{\partial \rho_1}{\partial Y} = \sum_{k,l;s} \frac{\partial}{\partial H_{kl;s}} \left[\frac{\partial}{\partial H_{lk;s}} + \gamma H_{kl;s} \right] \rho_1 \quad (\text{A1})$$

where Y is given by eq.(7), $\rho_1 = C_2 \rho = \frac{C_2}{C} \tilde{\rho}$ (with C as a normalization constant such that $\int \tilde{\rho} DH = 1$ and C_2 as a function of $y_{kl;s}$, $x_{kl;s}$, discussed in *appendix A* of [1]).

The above equation along with eq.(3) in turn leads to a Y governed evolution of \tilde{P}_e (details discussed in *appendix B* of [1] and also in [2]),

$$\frac{\partial P_1}{\partial Y} = \sum_{s=1}^2 \sum_{n=1}^N \frac{\partial}{\partial z_{ns}} \left[\frac{\partial}{\partial z_{ns}} - 2 \frac{\partial \ln |\Delta_N(z)|}{\partial z_{ns}} + \gamma z_{ns} \right] P_1 \quad (\text{A2})$$

with $P_1(z_1, \dots, z_N)$ related to the normalized distribution by $\tilde{P}_e = C_2 P_1 / C$, with $\Delta_N(z) \equiv \prod_{k < l}^N (z_k - z_l)$.

An integration of eq.(A2) over the variables z_{n+1}, \dots, z_N (as well as their conjugates), multiplying both sides by $\frac{N!}{(N-n)!}$ and subsequently using eq.(4) leads to four types of terms given as follows.

$$\frac{N!}{(N-n)!} \int \frac{\partial P_1}{\partial Y} D\Omega_{n+1} = \frac{\partial R_n}{\partial Y}, \quad (\text{A3})$$

and

$$\begin{aligned} \frac{N!}{(N-n)!} \int \frac{\partial^2 P_1}{\partial z_{jr}^2} D\Omega_{n+1} &= \frac{\partial^2 R_n}{\partial z_{jr}^2} \quad j \leq n, \\ &= 0 \quad j > n, \end{aligned} \quad (\text{A4})$$

with $D\Omega_{n+1} \equiv d^2 z_{n+1}, \dots, d^2 z_N$ with $d^2 z \equiv dz d^* z$.
Similarly

$$\begin{aligned} &\frac{N!}{(N-n)!} \int \frac{\partial}{\partial z_{jr}} (\ln |\Delta_N(z)| P_1) D\Omega_{n+1} = 0 \quad j > n, \\ &= \frac{\partial}{\partial z_{jr}} (\ln |\Delta_n(z)| R_n) \quad i, j \leq n, \\ &= \frac{1}{N-n} \sum_{j,r} \frac{\partial}{\partial z_{jr}} \int \frac{z_{jr} - z_{n+1r}}{|z_j - z_{n+1}|} R_{n+1}(z) d^2 z_{n+1} \quad i > n, j \leq n, \end{aligned} \quad (\text{A5})$$

with $R_{n+1}(z) \equiv R_{n+1}(z_1, \dots, z_{n+1})$. and

$$\begin{aligned} \frac{N!}{(N-n)!} \int \frac{\partial}{\partial z_{jr}} (z_{jr} P_1) D\Omega_{n+1} &= \frac{\partial}{\partial z_{jr}} (z_{jr} R_n), \quad j \leq n, \\ &= 0 \quad j > n. \end{aligned} \quad (\text{A6})$$

Using the above relations then leads to eq.(5).

Appendix B: Nearest Neighbor Spacing Distribution (NNSD)

A nearest neighbor spacing $S_{1,k}$ for an unfolded eigenvalue e_k is defined as $|e_k - e_\alpha|$ with e_α as the nearest eigenvalue to e_k on the complex plane: $S_{1,k} = \min_\alpha |e_k - e_\alpha|$. Due to ease of measurement, the spectral analysis through experimental as well as numerical route is often based on the distribution $P(S, e)$ of unfolded nearest neighbor spacings S at spectral point e and thus a measure for short range correlations. While $R_2(S; e)$ in general depends on the eigenvalue spacings S of all orders, it is approximately same as $P(S; e)$ for small S . (Indeed, as in case of a real spectrum, \mathcal{R}_2 can be expressed as a sum over k^{th} order spacing distributions $P_k(S; e)$:

$$\mathcal{R}_2(S, e) = \sum_{k=0}^{\infty} P_k(S, e) \quad (\text{B1})$$

with $P_0 \equiv P$ as the nearest neighbor spacing distribution [54]). Using the above relation in eq.(17) then implies that the evolution of $P_k(S, e)$ with changing system conditions and from an arbitrary initial condition is governed by Λ_e too for all k including $k = 0$.

With changing system conditions, the eigenvalues distribution on a complex plane for many non-Hermitian systems undergoes a variation between two extremes, namely, uncorrelated eigenvalues (Poisson universality class) and correlated eigenvalues through mutual repulsion (Ginibre universality class). For the former, $P(S; e)$ is the 2-dimensional Poisson distribution, independent of e :

$$P(S) = 2c_p S e^{-\alpha_p S^2} \quad (\text{B2})$$

with c_p and α_p determined from the normalization condition $\int_0^\infty P(S) dS = 1$ and the unit mean level spacing condition $\int_0^\infty S P(S) dS = 1$. For the Ginibre ensemble of complex matrices, the spacing distribution $P(S; e)$ (independent of e) is [16]:

$$P(S) = c_g P_g(c_g S) \quad (\text{B3})$$

with

$$P_g(S) = \lim_{N \rightarrow \infty} \left[\prod_{n=1}^{N-1} f_n(S^2) e^{-S^2} \right] \left[\sum_{n=1}^{N-1} \frac{2S^{2n+1}}{n! f_n(S^2)} \right] \quad (\text{B4})$$

and

$$f_n(x) = \sum_{m=0}^n \frac{x^m}{m!} = e^x - \sum_{m=n+1}^{\infty} \frac{x^m}{m!} \quad (\text{B5})$$

and with c_g as the mean level spacing $\int_0^\infty S P_g(S) dS \approx 1.1429$.

From eq.(B5), $f_n(x)$ for $S < 1$ limit can be approximated as $f_n(x) \sim 1$. This in turn gives, for small- S , $P(S) = (1/2) c_g^3 S^3 e^{-c_g^2 S^2}$. For large $S(> 1)$, $f_n(x)$ can be approximated by its dominant term $f_n(x) \sim \frac{x^n}{n!}$. This in turn gives the dominant contribution from the second bracket in eq.(B4) as S and from the first bracket as $\left(\prod_{n=1}^{N-1} \frac{S^{2n}}{n!}\right) e^{-S^2}$. For $S > 1$, eq.(B4) can then be approximated as $P(S) \sim S \left(\prod_{n=1}^{N-1} \frac{c_g^{2n} S^{2n}}{n!}\right) e^{-c_g^2 S^2}$ or simply as $P(S) \sim e^{-c_g^2 S^2}$ (with exponential term dominating over powers of S).

Appendix C: Spacing Ratio Distribution

For a meaningful comparison of the statistics of two different ensembles or even those for a same ensemble at two different spectral locations, it is necessary to rescale the spectrum by $R_{1,local}(e)$. This however requires a prior knowledge of $R_{1,local}(e)$ which is often not known for non-stationary ensembles and the standard route is to determine it through numerical calculation. Besides, in case $R_1(e)$ is not a smooth function of energy, the unfolding procedure becomes non-trivial even if $R_1(e)$ is analytically known and the spectrum is locally stationary. Indeed as almost all standard spectral fluctuation measures e.g nearest neighbour spacing distribution and number variance are sensitive to unfolding issues, it is preferable to consider a dimensionless measure e.g. the nearest neighbour spacing ratio. For real spectrum, the measure is defined as [59] $P(r) = \sum_{i=1}^{N-1} \langle \delta(r - r_i) \rangle$ with r defined as the ratio of consecutive spacings between nearest neighbour levels: $r_i = S_{i+1}/S_i$ where $S_i = e_{i+1} - e_i$ is the distance between two nearest neighbour eigenvalues. As the ratio r does not depend on the local density of states, an unfolding of the spectrum for $P(r)$ is not required. Further $P(r)$ being a short range fluctuation measure, the probability of error due to mixing spectral statistics is reduced.

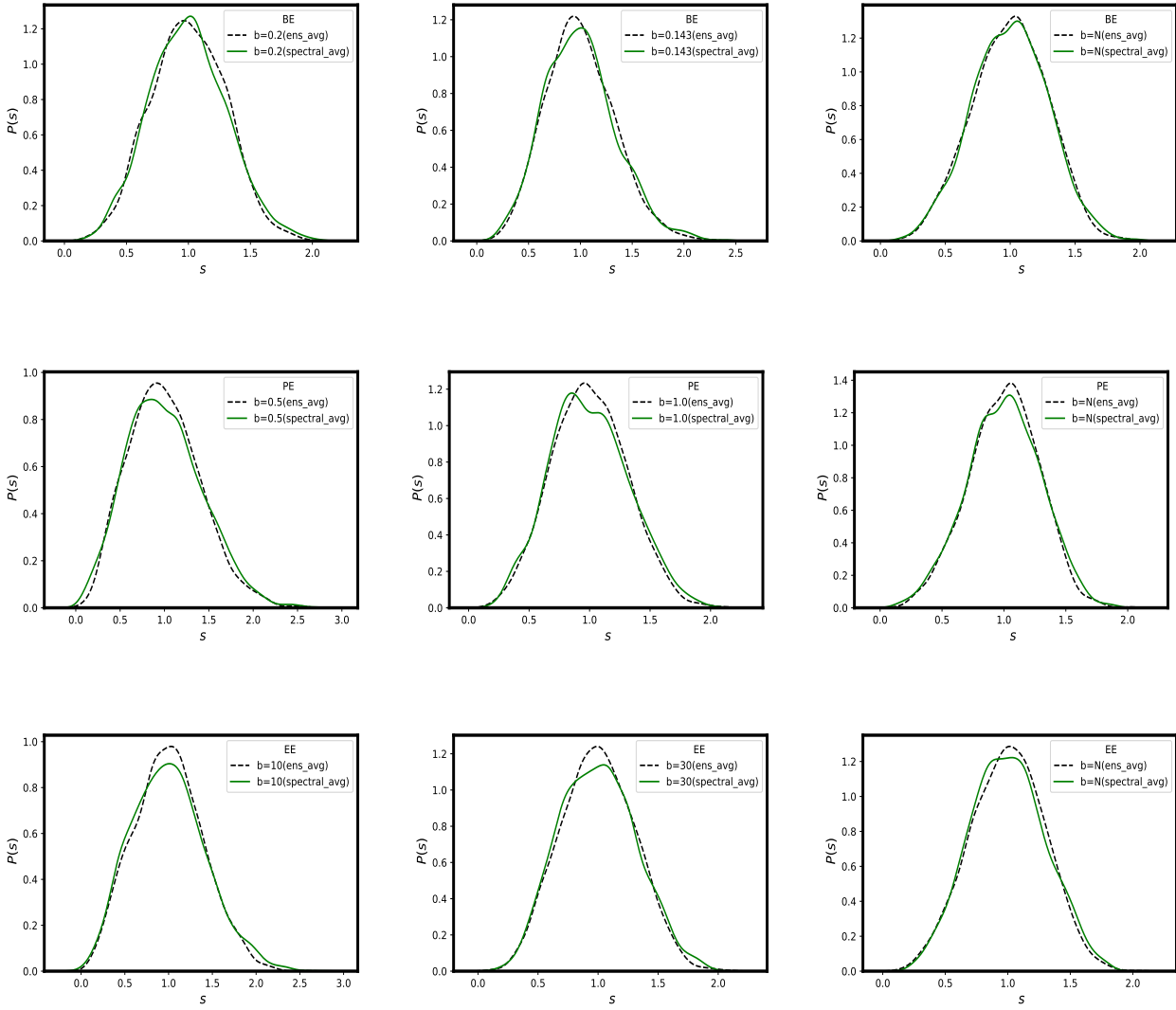


FIG. 1. **Local ergodicity of the spectral fluctuations on the complex plane:** The figure displays a comparison of $P(S) \equiv P_e(S, e; \Lambda_e)$ obtained by ensemble averaging with that of spectral-ensemble averaging for three different b -values for each ensemble (i.e BE, PE and EE). The ensemble averaging is obtained by choosing a single spacing (equivalently at a single spectral point) near $z \sim 0$ and averaging over an ensemble of 2500 matrices each of size $N = 1024$. The spectral-ensemble averaging is carried out by averaging over a few spacings (~ 100) within a range Δz around $z \sim 0$ from each matrix as well as over the ensemble of 25 matrices; the total number of spacings is same for both the cases. As the visuals indicate, the two averages are almost analogous.

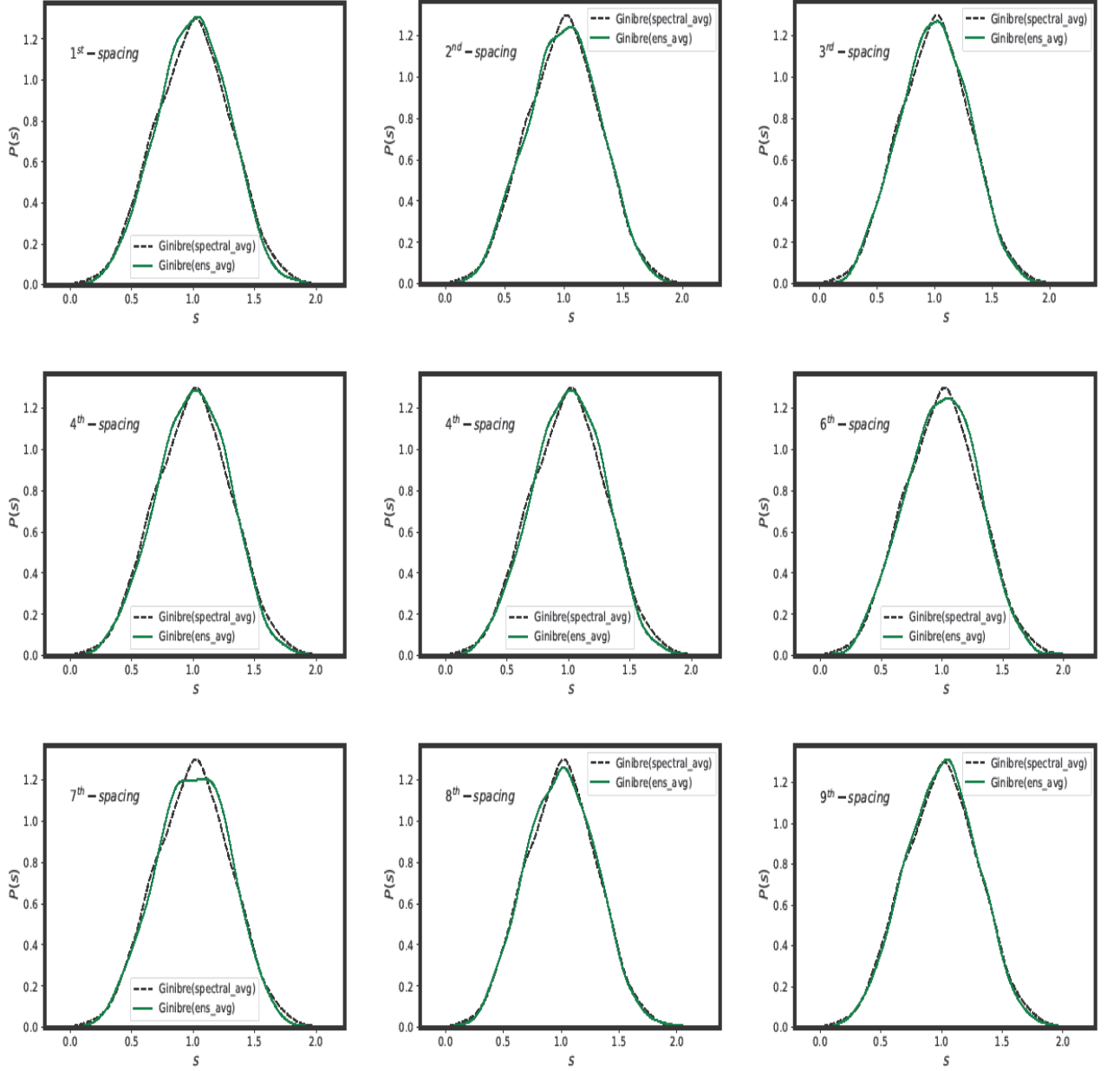


FIG. 2. **Ergodicity of the spectral fluctuations on the complex plane for Ginibre ensemble** : The figure displays a comparison of $P(S) \equiv P_e(S, e; \infty)$ obtained by ensemble averaging with that of spectral averaging, for different choice of single spacings i.e different e values. The details of the two averaging procedure are same as in figure 1. The two averages almost overlap in each case, irrespective of the choice of the single spacing used for the ensemble averaging.

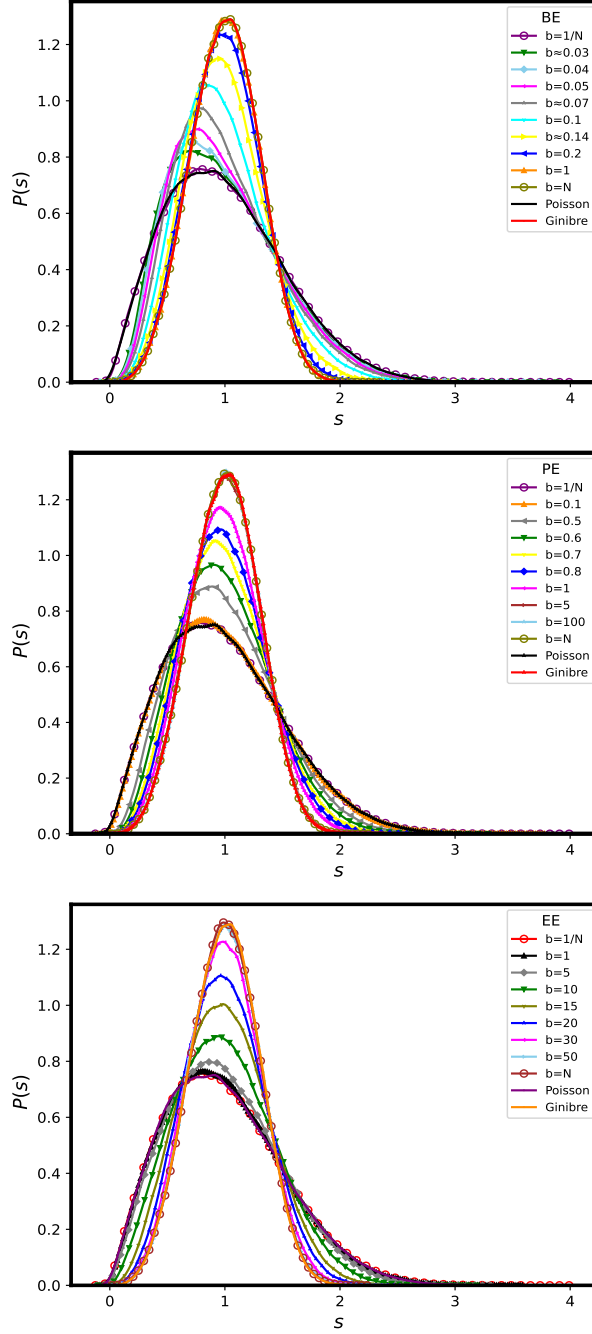


FIG. 3. **Single parameter governed evolution of the fluctuation measures:** The figure displays the spectral-ensemble averaged nearest neighbour spacing distribution $P(S) \equiv P_e(S, e; \Lambda_e)$ of the eigenvalues on the complex plane (10% taken from the neighborhood for $e \sim 0$) for many b values while N is kept fixed ($N = 1024$) for the three ensembles, each consisting of 2500 matrices. As can be seen from the figure, a smooth crossover from Poisson to Ginibre limit occurs for each case as b and thereby Λ_e varies. A slight shift of the peak towards left for BE cases seems to be an artefact of the unfolding issues. A good agreement of $P(S)$ for finite Λ_e with eq.(26) is displayed in figure 4 (the comparison displayed in a separate figure for the purpose of clarity).

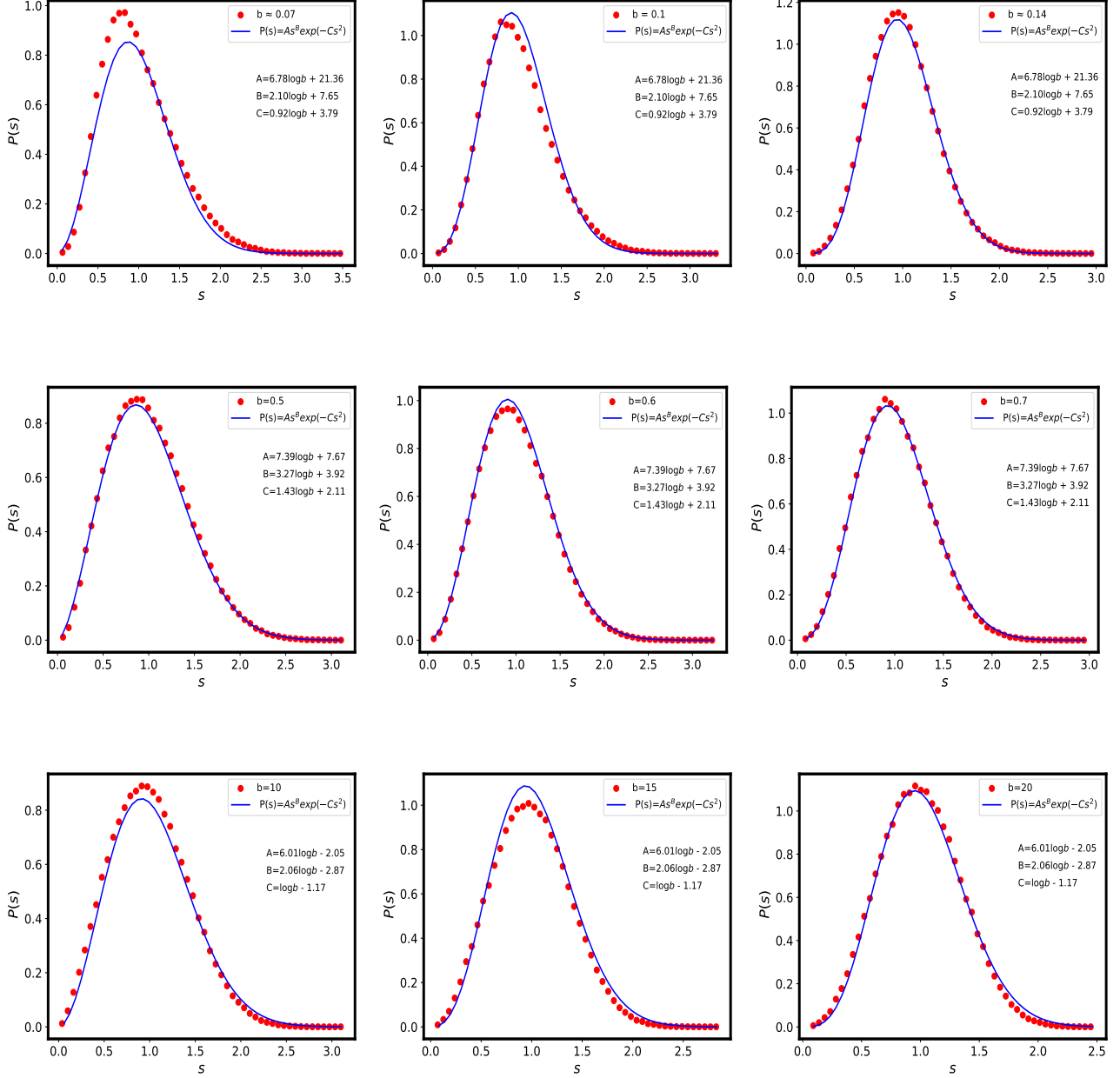


FIG. 4. $P_e(S, e; \Lambda_e)$ for finite Λ_e : comparison with theoretical conjecture eq.(26): The figure displays a comparison with eq.(26) of the $P(S) \equiv P_e(S, e; \Lambda_e)$ many b values and a fixed $N = 1024$ for the three ensembles, each consisting of 2500 matrices. As given in table 1, the fitted parameters A, B, C can be recast as the functions of Λ_e . Here again the definition $\Lambda_e = \log b - C$ as the crossover parameter seemingly apply quite well.

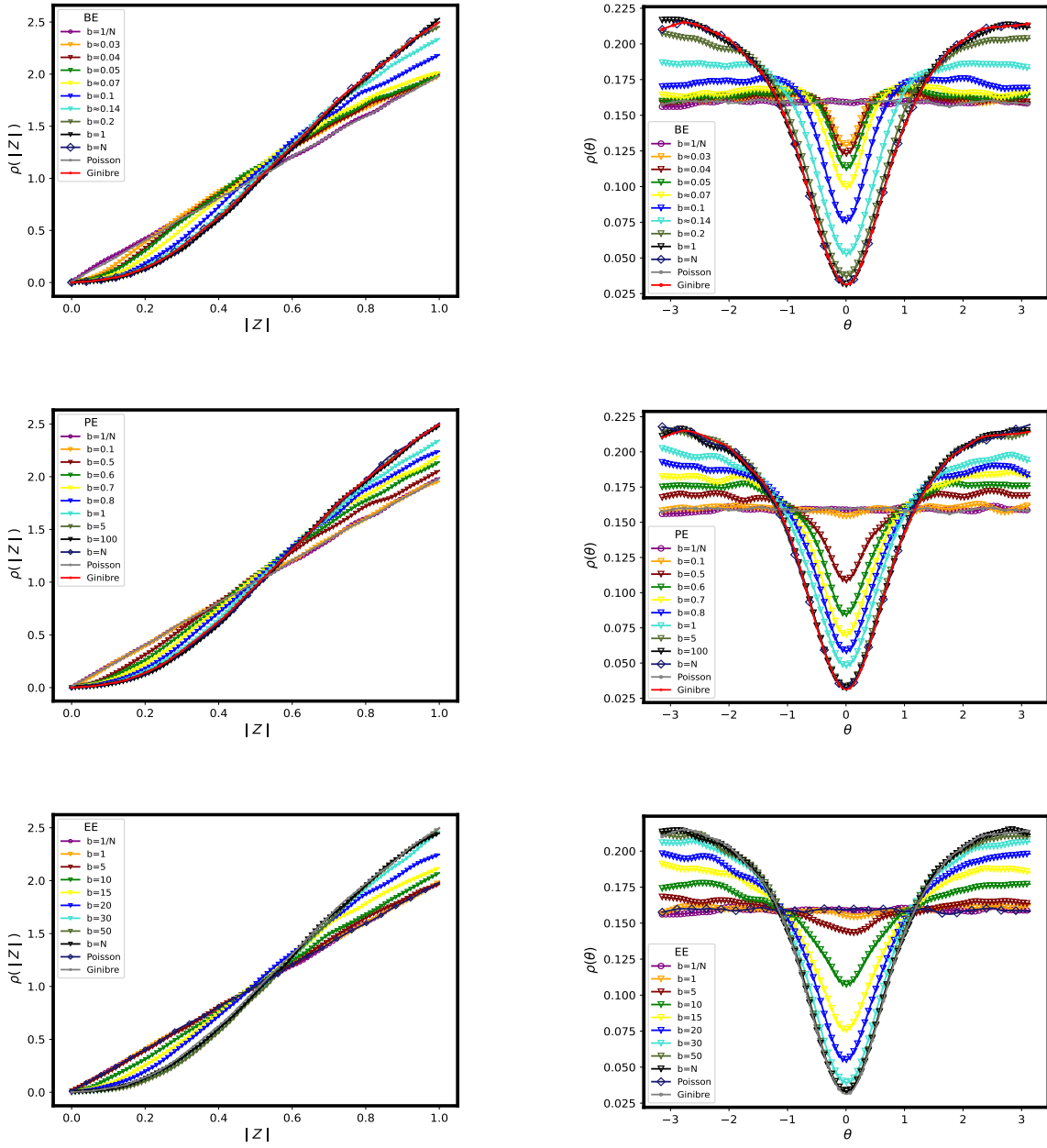


FIG. 5. **Radial and angular dependence of spacing ratios:** Figure illustrates the radial $\rho(|z|)$ and angular parts $\rho(\theta)$ of the spectral-ensemble averaged nearest neighbour spacing distribution $P_z(z)$ with $z = |z|e^{i\theta}$ on the complex plane for many b values for fixed system size $N = 1024$ and ensembles size $M = 5000$. As shown in left panels of figure, while $\rho(|z|)$ for intermediate b values lies between Poisson and Ginibre limit in both regions $|z| < 0.5$ and $|z| > 0.5$, they seemingly converge to same point in the neighborhood of $|z| \sim 0.5$. The display in right panel confirm the almost homogeneous $\rho(\theta)$ distribution in Poisson limit for each ensemble but it rapidly changes with increasing b . Indeed $\rho(\theta)$ approaches a minimum for $\theta = 0$ as b approaches Ginibre limit. This indicates that increasing level repulsion among consecutive eigenvalues with increasing b causes them to lie at large angular separations.

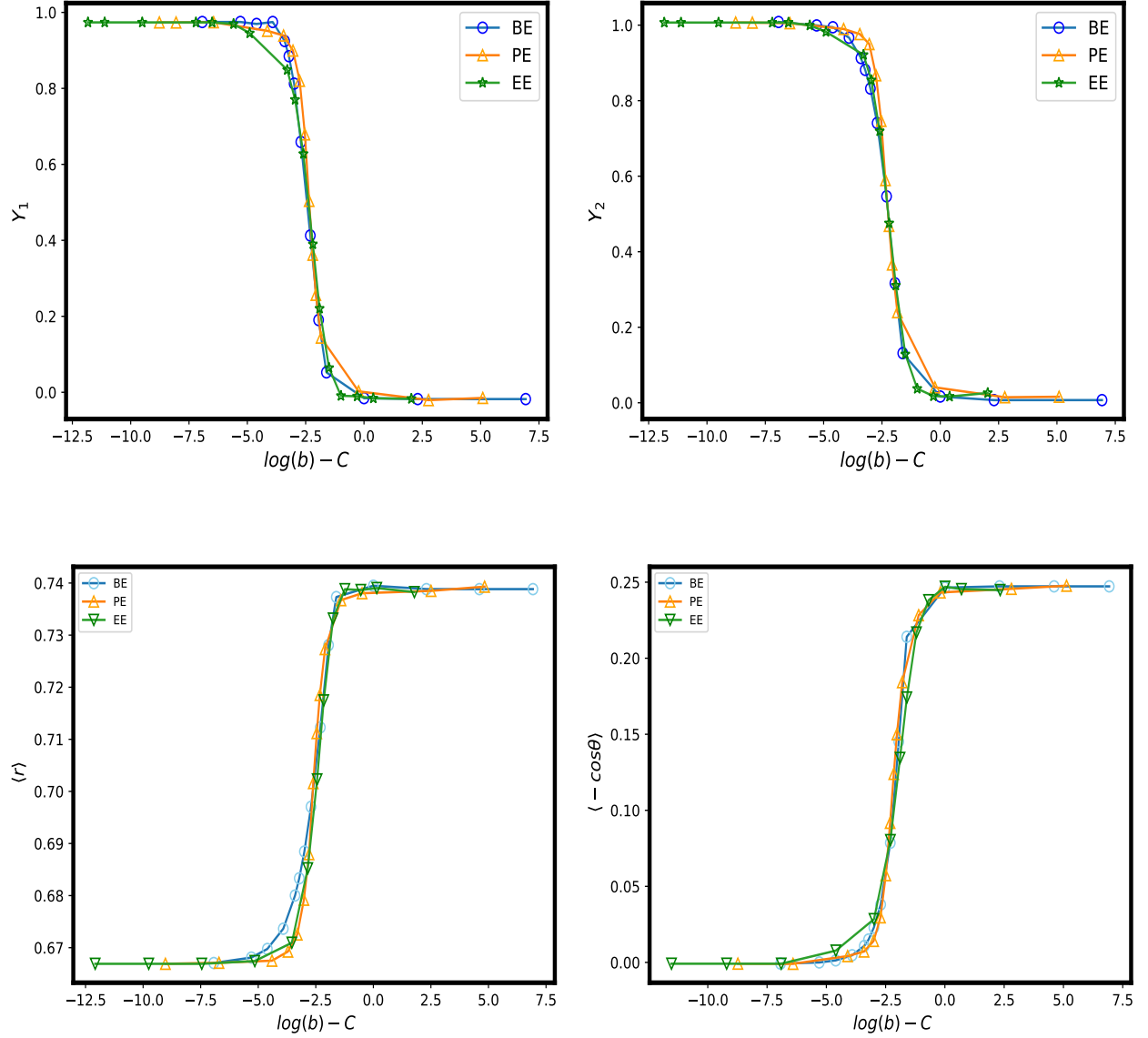


FIG. 6. Universality of local fluctuations in non-stationary non hermitian ensembles: The figure displays the behavior of four different fluctuation measures, namely, (i) $\gamma(x_1)$, (ii) $\gamma(x_2)$, (iii) $\langle r \rangle$, (iv) $-\langle \cos \theta \rangle$ on the complex spectral plane, with $x_1 = 0.656978$ and $x_2 = 1.446259$. As can be seen from the figure, the behavior of each measure vs $\log b - c$ for three ensembles collapses onto same curve, with $c = 0, 1.8, 4.6$ for BE, PE and EE respectively. An important point worth noting is the rapid transition of each measure from one extreme limit to another, indicating a critical statistics near $\log b - c \approx -2$.

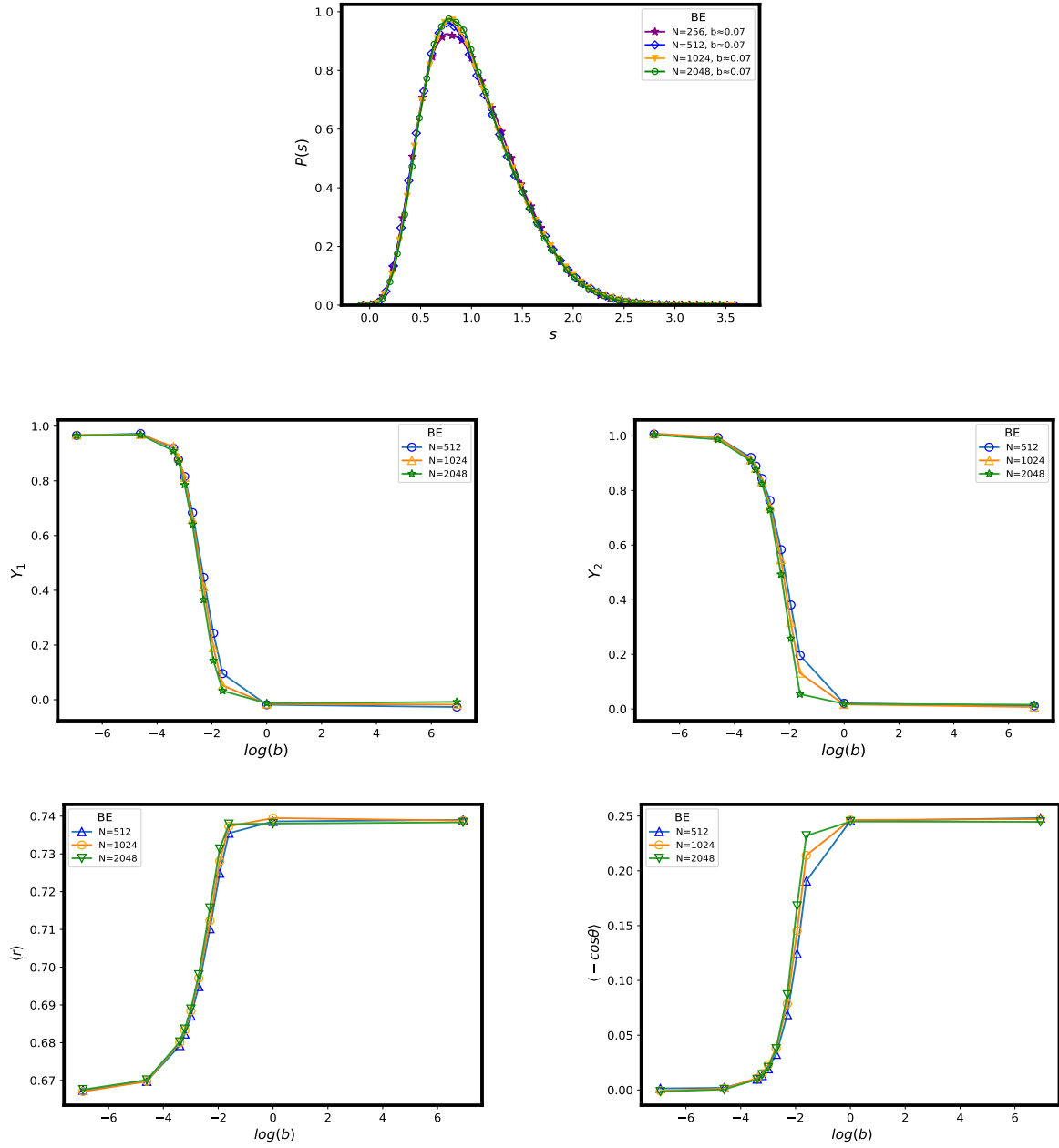


FIG. 7. **Critical BE Statistics** The figure displays the statistical behavior for BE at critical values of the ensemble parameters (given in eq.(18)) based on following fluctuation measures: (i) $P(S)$, (ii) γ_1 , (iii) γ_2 , (iv) $\langle r \rangle$, (v) $-\langle \cos \theta \rangle$. As can be seen from each parts of the figure, the statistics for each measure remains invariant with changing N for entire range of b . This indicates the criticality of the ensemble for chosen set of the ensemble parameters. More clearly the spectral statistics near $e \sim 0$ is critical irrespective of the b and N values if the variances of the diagonal are taken in a specific combination described in eq.(18).

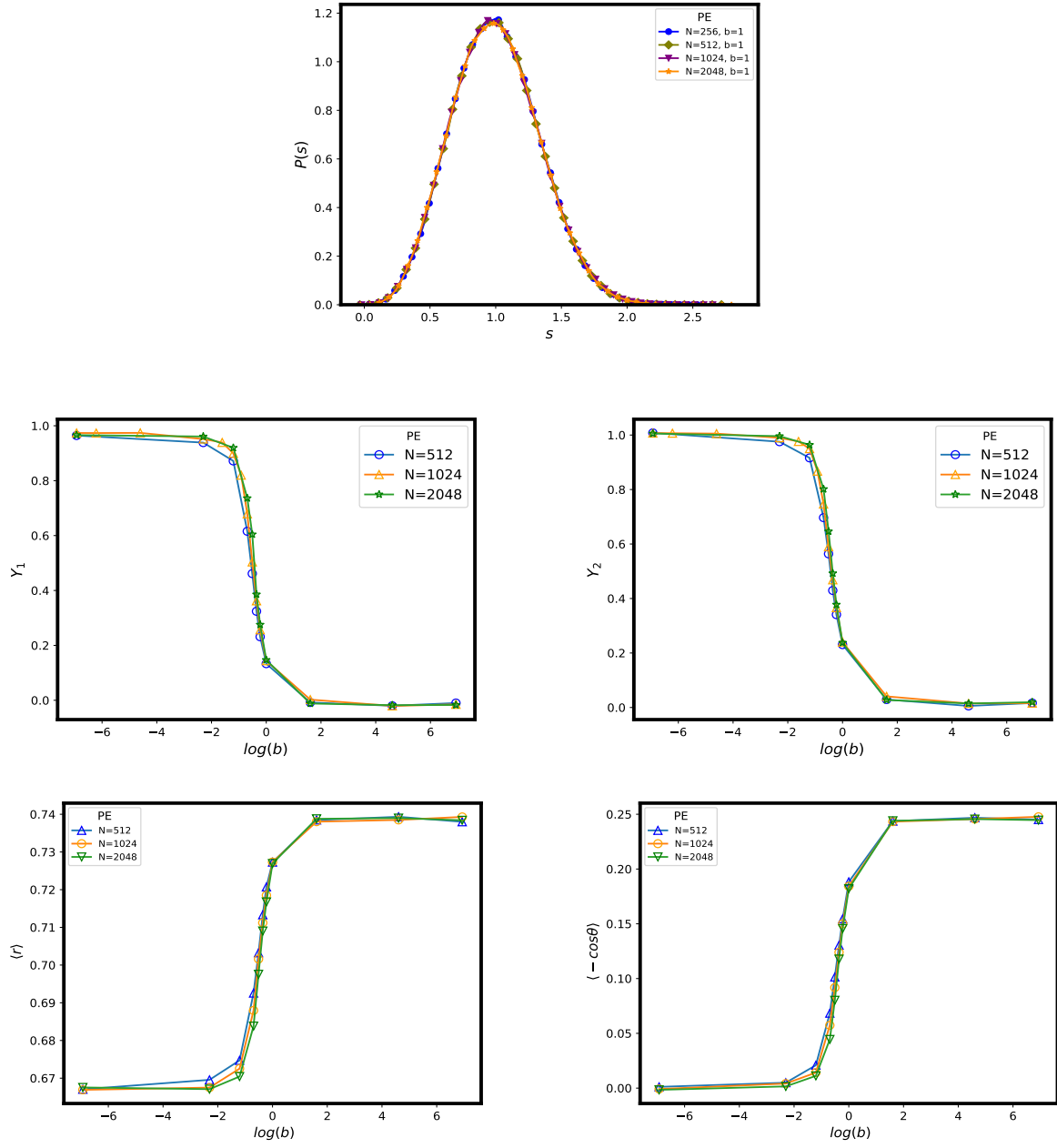


FIG. 8. **Critical PE Statistics:** the details here are same as in figure 7 except now the critical PE ensemble is described by eq.(19).

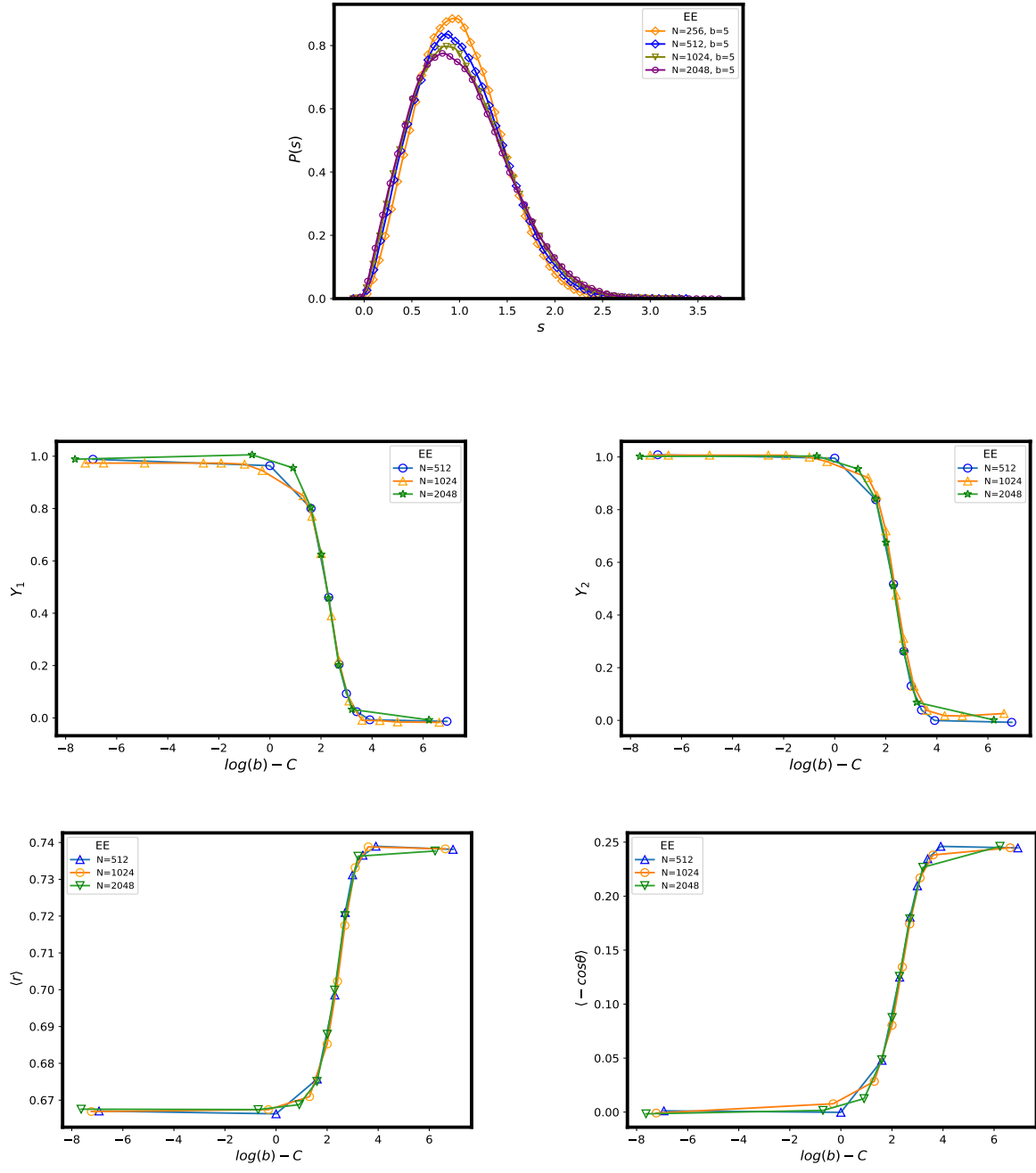


FIG. 9. **Critical EE Statistics:** The details here are same as in figure 7 except now the critical EE ensemble is described by eq.(20).